

NUMERICAL MODELING OF PARAMETRIC UNCERTAINTIES
IN FLOW THROUGH POROUS MEDIA: DEVELOPMENT
AND INITIAL TESTING OF PORSTAT

Budhi Sagar

Analytic and Computational Research, Inc.
Los Angeles, California 90066

Peter M. Clifton

Basalt Waste Isolation Project
Rockwell Hanford Operations
Richland, Washington 99352

July 1983

Prepared for Rockwell Hanford
Operations, A Prime Contractor
to the U.S. Department of Energy
Under Contract DE-AC06-77RL01030

8311140362 831028
PDR WASTE
WM-10

PDR
Rec'd W/LTA DTD 8311140356 831028

Rockwell International
Rockwell Hanford Operations
Energy Systems Group
Richland, WA 99352

ACKNOWLEDGMENTS

The authors acknowledge the help and guidance given by personnel from Analytic and Computational Research, Inc. (ACRI), Rockwell Hanford Operations (Rockwell), and Boeing Computer Services, Richland (BCSR). Dr. Akshai K. Runchel (ACRI) was the senior author of the original version of PORFLO, which is the precursor of PORSTAT, and he provided help and guidance during this study. Mr. Clement K. Tam (ACRI) performed some of the computer code modification required to produce PORSTAT and assisted in the running of the test cases. Dr. Raul A. Deju, Director, Basalt Waste Isolation Project, and Messrs. Ronald C. Arnett and Robert G. Baca (Rockwell) reviewed the report and provided many suggestions that improved the quality of the final manuscript. Mr. Niall W. Kline (BCSR) contributed with technical discussions. Mr. James L. Cheshire (Rockwell) provided the administrative interface between ACRI and Rockwell during the study.

ABSTRACT

The Basalt Waste Isolation Project (BWIP) is one of the major research projects being conducted under the National Waste Terminal Storage Program, which was initiated to investigate the feasibility of storing high-level nuclear waste in deep rock formations. The Basalt Waste Isolation Project is currently investigating the deep basalts beneath the U.S. Department of Energy's Hanford Site for location of a high-level nuclear waste repository.

A major part of BWIP's current effort is directed at analyzing post-closure repository performance. These analyses will determine how well the proposed repository system achieves its design objectives, and, in turn, how well the system complies with technical criteria and standards set by Federal agencies.

Previous performance analyses conducted by BWIP generally have been carried out in a deterministic framework, whereby a single model prediction was made and nothing was known about the likelihood of that prediction. As the size of the data base used for repository performance analyses increases, BWIP will progressively move toward a stochastic approach to performance studies. The main advantages of a stochastic approach are that: 1) the likelihood of model predictions can be quantified, and 2) information can be gained about how to reduce the uncertainty in these predictions.

This report documents the development and initial testing of the computer code PORSTAT. PORSTAT solves the stochastic groundwater flow equation coupled with the deterministic heat transfer and mass transport equations. An integrated finite-difference numerical scheme is used in PORSTAT to solve the governing equations. The stochastic groundwater flow equation is approximated by means of a second-order uncertainty analysis technique. Stochastic variables input to PORSTAT may be hydraulic conductivity, specific storage, boundary conditions, and initial conditions. The output from PORSTAT consists of the expected values and covariances of hydraulic heads and Darcian velocities. PORSTAT will be used by BWIP to stochastically model groundwater flow in the thermally influenced zone around the repository.

In order to make a preliminary evaluation of PORSTAT's ability to solve the stochastic groundwater flow equation, the results from two test cases run by PORSTAT and BWIP's Monte Carlo groundwater flow computer code (MAGNUM-MC) are compared. The initial comparison indicates that PORSTAT tends to overestimate the uncertainty in hydraulic head predictions, and thus from a risk analysis viewpoint, produces conservative results. Additional testing is being conducted to determine the limitations and capabilities of PORSTAT.

CONTENTS

1.0	Introduction	1
1.1	Background	1
1.2	Study Organization	3
2.0	Technical Review	3
2.1	Uncertainties in Model Predictions	3
2.2	Review of Groundwater Flow Uncertainty Analysis Methods	4
2.3	The Adjoint Method of Sensitivity Analysis	6
3.0	Mathematical Basis of PORSTAT	7
3.1	Governing Equation for Groundwater Flow	7
3.2	Governing Equations for Temperature and Mass Transport	9
3.3	Discretization of the Groundwater Flow Equation	9
3.3.1	The Grid: The Point-Centered Grid System	9
3.3.2	Discretization: Method of Nodal Point Integration	12
3.3.3	Incorporation of Boundary Conditions	12
3.3.4	Formation of Random Equations	13
3.4	Theory of Second-Order Analysis	13
3.4.1	Concept of Solution of Random Algebraic Equations	13
3.4.2	Principal of Second-Order Analysis	13
3.5	Evaluation of First- and Second-Order Derivatives	15
3.6	Expected Value and Covariance of Darcian Velocity	16
3.7	Summary and Discussion	16
4.0	Application of PORSTAT to Test Cases	17
4.1	Test Case 1	17
4.1.1	Physical Description and Grid System	17
4.1.2	Stochastic Hydraulic Conductivity Data	18
4.1.3	Results	19
4.2	Test Case 2	22
4.2.1	Physical Description and Grid System	22
4.2.2	Stochastic Hydraulic Conductivity Data	22
4.2.3	Results	22
5.0	Summary and Conclusions	30
6.0	References	31
Appendices:		
A.	Equations for Sensitivity Coefficients	A-1
B.	Equations for Second-Order Derivatives	B-1
C.	Equations for Covariance of Darcian Velocities	C-1
D.	Monte Carlo Technique for Analyzing Uncertainties in Hydraulic Heads	D-1
E.	Hydraulic Conductivity Field Mean Vector and Covariance Matrix Generation, Test Case 1	E-1

Appendices: (Contd)

F.	Hydraulic Conductivity Field Mean Vector and Covariance Matrix Generation, Test Case 2	F-1
G.	Derivation of the Mean Vector and Covariance Matrix of a Log-Normally Distributed Random Variable Given the Mean Vector and Covariance Matrix of the Corresponding Normally Distributed Random Variable	G-1

FIGURES:

1.	Location of the Hanford Site	2
2.	Example of Point Centered Grid System	10
3.	A Typical Grid Cell	10
4.	Grid System and Boundary Conditions Input to PORSTAT, Test Case 1	18
5.	Standard Deviation of Hydraulic Head Computed by PORSTAT, Test Case 1	19
6.	Hydraulic Head Correlation Structure From Node 1, Test Case 1	23
7.	Hydraulic Head Correlation Structure From Node 17, Test Case 2	23
8.	Expected Values of Hydraulic Conductivity Input to PORSTAT, Test Case 2	24
9.	Standard Deviation of Hydraulic Conductivity Input to PORSTAT, Test Case 2	24
10.	Deterministic Hydraulic Head Field Computed by PORSTAT, Test Case 2	25
11.	Standard Deviation of Hydraulic Head Computed by PORSTAT, Test Case 2	27
12.	Hydraulic Head Correlation Structure From Node 1, Test Case 2	29
13.	Hydraulic Head Correlation Structure From Node 17, Test Case 2	29

TABLES:

1.	Deterministic Solution and Expected Values of Hydraulic Head, Test Case 1	20
2.	Standard Deviation of Hydraulic Head, Test Case 1	21
3.	Deterministic Solution and Expected Values of Hydraulic Head, Test Case 2	26
4.	Standard Deviation of Hydraulic Head, Test Case 2	28

1.0 INTRODUCTION

The National Waste Terminal Storage (NWTs) Program was initiated in the mid-1970's for the purpose of investigating the feasibility of storing nuclear wastes in deep rock formations. A number of rock types (e.g., salt, granite, tuff, and basalt) were initially studied on a generic basis to assess their general suitability for nuclear waste storage. As studies progress, the NWTs Program is moving toward the identification and characterization of candidate repository sites. The Nuclear Waste Policy Act of 1982 provides legislative guidelines for nuclear waste repository site selection, design, licensing, construction, and operation.

1.1 BACKGROUND

The Basalt Waste Isolation Project (BWIP) is one of the major research and development projects being conducted under the NWTs Program. Rockwell Hanford Operations (Rockwell), a prime contractor to the U.S. Department of Energy (DOE), is currently responsible for the BWIP investigations. These investigations will eventually determine if high-level nuclear waste can be safely stored in the deep basalts beneath DOE's Hanford Site in south-central Washington State (Fig. 1). In a broad sense, BWIP's mission is to identify a potential repository site and develop the technology required for permanent isolation of radioactive wastes in the basalt formations (Deju, 1982).

Field investigations by BWIP are focusing on the geologic and hydrologic characterization of the Columbia River Basalt Group in the vicinity of the Hanford Site. The Columbia River Basalt Group is composed of a monotonous sequence of basalt flows that are occasionally separated by sedimentary interbeds in the upper part of the sequence. Formations belonging to this basalt group are known to have a cumulative thickness exceeding 3,000 m in some locations beneath the Hanford Site. Individual basalt flows may be as thick as 70 m and laterally continuous for many kilometers (Myers/Price et al., 1979). Although basalt characteristically is a fractured rock, field studies have shown that the dense interiors of deep basalt flows typically have relatively low permeabilities (Gephart et al., 1979; Rockwell, 1982). These relatively low permeabilities are most likely due to the high lithostatic load at depth and secondary mineralization of fractures (Spane, 1982).

A major part of BWIP's current effort is directed at analyzing post-closure repository performance. These analyses will show how well a proposed repository system achieves its design objectives, and, in turn, how well the system complies with performance criteria set by Federal agencies. A performance analysis usually is conducted by applying a suite of mathematical models to geologic, hydrologic, and geochemical data.

Previous performance analyses reported by Rockwell generally have been carried out in a deterministic framework (Rockwell, 1982). Such analyses use "best estimates" of model input parameters in order to obtain the corresponding "best estimates" of the model outputs (or state variables). Deterministic models have also been used to examine the impact of postulated disruptive events on repository performance (Arnett et al., 1980). One problem

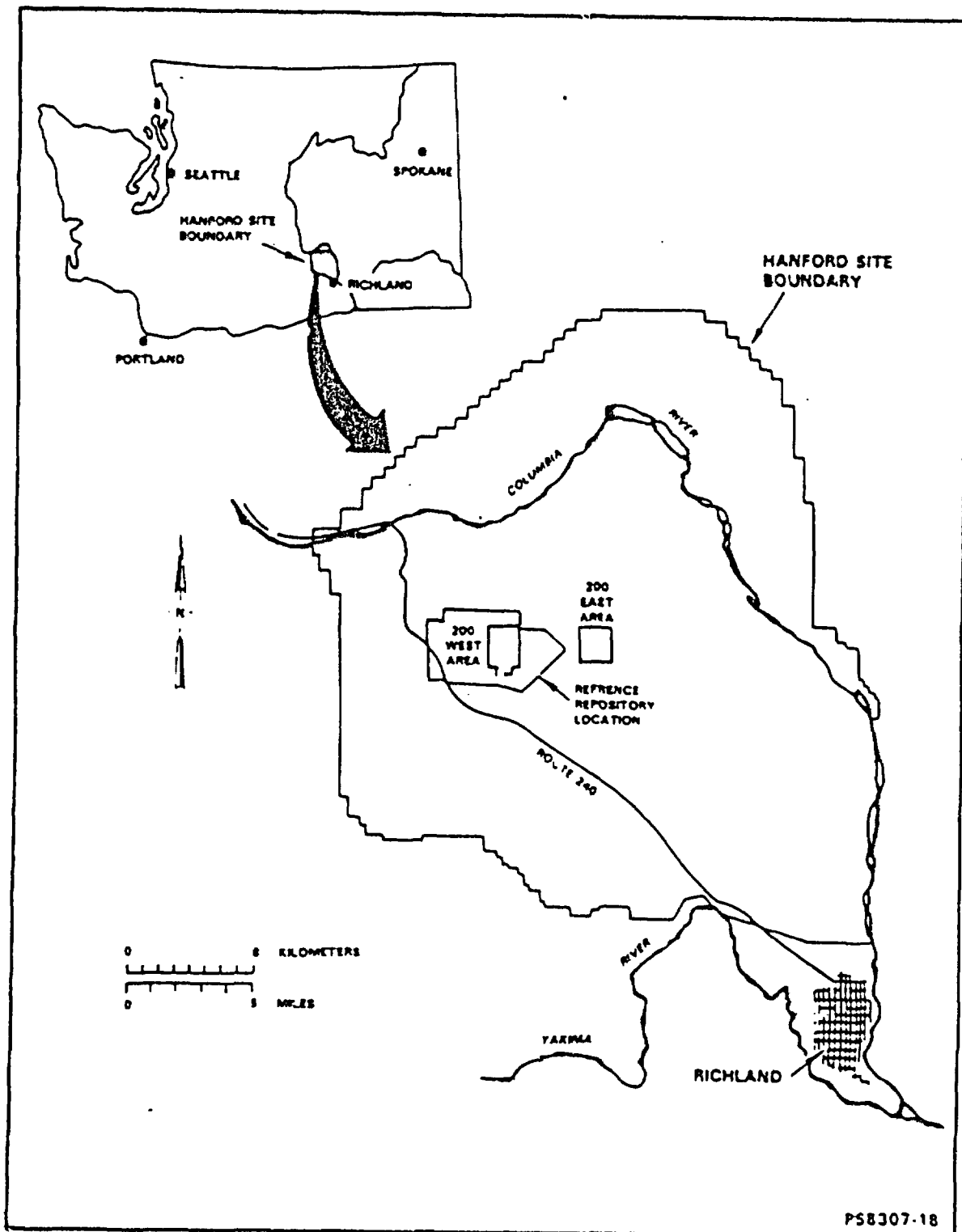


FIGURE 1. Location of the Hanford Site.

with deterministic analyses is that the likelihood of the model output may be difficult to quantify unless some statistically based method was used to develop the model input. This is especially true when deterministic models are used to examine the impacts of postulated disruptive events.

In order to quantify the uncertainty in repository performance predictions, a stochastic approach to performance studies must be adopted. With a stochastic model, part or all of the input parameters and/or boundary conditions are considered uncertain, and thus the output is also uncertain and must be described by statistical measures such as means, variances, and covariances. In general, it is desirable to use stochastic modeling when the data base becomes large enough so that uncertainties in model inputs can be quantified.

This report describes the development and initial testing of the computer code PORSTAT. PORSTAT has been developed from PORFLO, which is the computer code being currently used by BWIP to model coupled groundwater flow, heat transfer, and mass transport in the near-field repository environment. (PORFLO was developed by Analytic and Computational Research, Inc. for Rockwell.) In contrast to PORFLO, however, PORSTAT solves the stochastic groundwater flow equation coupled with the deterministic heat transfer and mass transport equations. It was decided to stochastically treat only the groundwater flow equation in this study because, in the case of data from the basalts beneath the Hanford Site, uncertainties generally are largest in the parameters that need to be specified in order to solve this equation. The development of PORSTAT will give BWIP the capability of stochastically modeling groundwater flow in the near-field environment of a repository in basalt.

1.2 STUDY ORGANIZATION

The study reported in this document was carried out as a joint effort between the staffs of Analytic and Computational Research, Inc. and Rockwell. Analytic and Computational Research, Inc. assumed the lead role in formulating the stochastic groundwater flow equation and suitably modifying PORFLO to become PORSTAT. Rockwell developed the test cases used to provide a preliminary evaluation of the ability of PORSTAT to solve the stochastic groundwater flow equation.

2.0 TECHNICAL REVIEW

2.1 UNCERTAINTIES IN MODEL PREDICTIONS

Predictions made by complex models of the types used in repository performance analyses will always have some associated uncertainty. By correctly applying a stochastic model, however, the amount of uncertainty in predictions can be quantified. Once this uncertainty is quantified, efforts can be made to reduce the uncertainty, if desired, by collecting more data or refining the model. Being able to quantify the uncertainty in predictions and indicate how these uncertainties may be reduced are major attributes of stochastic models.

In general, uncertainties in repository performance predictions are a consequence of the following:

- Limitations in the mathematical and numerical models (including computer codes) used to simulate repository performance
- Random and/or systematic measurement errors in the geologic, hydrologic, and hydrochemical data used to make parameter estimates for performance models
- Incomplete knowledge of the spatial or temporal structure of some of the data used to make parameter estimates for performance models (e.g., hydraulic conductivity)
- Heterogeneities within the hydrogeologic system that have not been detected during field investigations.

The first source of uncertainty, which can be termed model uncertainty, is examined when the computer codes used for performance predictions are benchmarked against other codes and verified with experimental data. The remaining three sources of uncertainty can be called data or parameter uncertainty and, for practical purposes, will always exist in repository performance studies. Theoretically, data uncertainties can be substantially reduced by densely sampling the model domain; however, some uncertainty will usually remain in data that vary with time. By using statistical methods such as those outlined by McLaughlin (1979), it is possible to quantify how data uncertainties impact model parameter estimates. Stochastic models can then be used to quantify the uncertainty in repository performance predictions.

2.2 REVIEW OF GROUNDWATER FLOW UNCERTAINTY ANALYSIS METHODS

At present, the methods being used in the state-of-the-art analysis of uncertainty of flow and mass transport in porous media can be broadly grouped into five categories:

1. Monte Carlo
2. Finite order
3. Perturbation
4. Analytic time or frequency domain
5. Stochastic Lagrangian.

Recently, the use of the Adjoint Method has been strongly suggested for the study of uncertainties associated with repository performance predictions (Thomas, 1982). The characteristics of this method are discussed in the next section.

The Monte Carlo technique is based on repetitive solution of the deterministic equations using parameter values derived by sampling the probability density functions of these parameters. This method has been used by Warren and Price (1961), Freeze (1975), Smith and Freeze (1979a, 1979b), and Clifton and Neuman (1982) to analyze groundwater flow, and by Smith and Schwartz (1980, 1981a, 1981b) to analyze mass transport in porous media. Monte Carlo methods have the advantage of being conceptually simple, and they are applicable to virtually all stochastic modeling problems. However, Monte Carlo methods have the disadvantage that the joint probability densities of all uncertain parameters must be specified. This may be impossible to do without gross assumptions being made if there are a large number of correlated parameters. In addition, the number of simulations required in order to assure convergence of the statistics of the model predictions depends on the number of uncertain parameters, the amount of uncertainty in each parameter, and the amount of correlation between parameters. By using sophisticated random sampling schemes such as Latin Hypercube Sampling (Iman et al., 1980) or stratified sampling (Ripley, 1981), it may be possible to reduce the number of simulations required to produce reliable statistics. Monte Carlo methods can, however, effectively result in an infinite-order uncertainty analysis.

The finite-order uncertainty analysis methods are based on the assumption that the solution space in the neighborhood of the expected values of the parameters is smooth and differentiable. The first-order method, which is the simplest of the finite-order methods, assumes that the solution space is linear in the neighborhood of the expected values of the parameters. Thus, only first-order derivatives of the solution with respect to the parameters need to be determined in a first-order uncertainty analysis. (In sensitivity theory, these derivatives are called "sensitivity coefficients.") The first-order derivatives are used together with the second statistical moment of the parameters to determine the second moment of the model predictions. The second-order uncertainty analysis method, which is to be used in this study, assumes that the solution space is at least of second degree in the neighborhood of the expected values of the parameters and that the first two derivatives of the solution with respect to the parameters exist. These derivatives together with the first two moments of the parameters are used to derive the first two moments of the model predictions. An implicit assumption used in applying a finite-order uncertainty analysis method is that any product containing either moments or derivatives of higher order than the order of the analysis is negligible. This assumption usually limits the application of low-order analyses (i.e., first or second order) to problems where the parameter uncertainties are not large. The actual limit of applicability of these methods has not as yet been defined in the literature. Finite-order uncertainty analyses of groundwater flow problems have been documented by Sagar (1978a) and Dettlinger and Wilson (1981).

The perturbation methods used by Tang and Pinder (1977, 1979), Oster et al. (1981), and Kincaid et al. (1983) are conceptually close to the finite-order uncertainty analysis methods. In the perturbation method, an array of equations containing moments of the parameters and model output is obtained by assuming that each uncertain variable can be represented by the sum of a deterministic part and a small random perturbation that has specified statistical moments. Generally, the set of equations obtained is open in the sense

that the number of equations is one less than the number of unknowns. In order to solve the set of equations, an assumption (called the closure assumption) is made whereby moments higher than a certain order are neglected.

Analytic time and frequency domain methods usually are applicable to simple problems where the uncertainties can be described by analytic functions. These methods have been used by Sagar (1978a, 1978b, 1979) in the time domain, and by Gelhar (1976), Bakr et al. (1978), and Gutjahr et al. (1978) in the frequency domain.

The stochastic Lagrangian methods of uncertainty analysis are based on tracking the motion of individual particles or groups of particles and then determining the statistics of the ensemble of particles at a specified time. These methods generally assume that the particles execute their motions independently of each other and that a probabilistic description of their velocities can be made. The random walk model of Ahlstrom et al. (1977) is an example of a stochastic Lagrangian model.

2.3 THE ADJOINT METHOD OF SENSITIVITY ANALYSIS

The application of the Adjoint Method (Oblow, 1978) to repository performance analysis studies has been strongly recommended in recent reports from the Office of Nuclear Waste Isolation (Thomas, 1982; Harper, 1983). It is instructive to remember that the utility of the Adjoint Method lies in evaluating, to a first-degree approximation, the first-order derivatives (sensitivity coefficients) of a specified scalar response function with respect to the model parameters. The Adjoint Method involves the solution of two sets of equations: primal and adjoint. In the context of the groundwater flow equation, the primal equations would be the set of simultaneous linear algebraic equations obtained after numerically approximating the governing partial differential equation. The adjoint set of equations is derived from the primal equations and the nature of the response being studied. In the case of the groundwater flow equation, the adjoint equations would also be a set of simultaneous linear algebraic equations. Examples of response functions that may be of interest in groundwater flow problems are the hydraulic head at one point in the flow domain or the mean hydraulic head in some region of the flow domain. While the primal set of equations is independent of the response function, a new set of adjoint equations is required each time the response function is redefined. Thus, if the response functions were the hydraulic heads at n points in space, the adjoint set of equations would have to be solved n times. In the case of a transient problem, these n equations would have to be solved at each time set.

Once the sensitivity coefficients have been computed by the Adjoint Method or any alternate method, they can be used in a first-order uncertainty analysis. However, the Adjoint Method does not estimate second- or higher-order derivatives of a response function with respect to model parameters. (These derivatives can be thought of as higher-order sensitivity coefficients.) At least second-order derivatives are required for the application of a second-order uncertainty analysis. An alternative to the Adjoint Method for computing sensitivity coefficients is described in this report. The

alternative method, which can compute both first- and second-order sensitivity coefficients, involves determining the explicit inverse of the matrix of the coefficients of the primal equations. The advantage this method has over the Adjoint Method is that once the inverse of the coefficient matrix is determined, the first- and second-order derivatives of all hydraulic heads with respect to all parameters are obtained in a single step. The disadvantage of this method is that both the coefficient matrix and its inverse are needed during computation, which requires storing both matrices. This may increase computer storage requirements significantly.

3.0 MATHEMATICAL BASIS OF PORSTAT

3.1 GOVERNING EQUATION FOR GROUNDWATER FLOW

The governing equation for groundwater flow in PORSTAT is based on the application of the principle of mass conservation together with the assumption that the flow dynamics under nonisothermal conditions are adequately described by the generalized form of Darcy's law. The equation so obtained is written below:

$$\frac{1}{r} \frac{\partial}{\partial x} (rK_x \frac{\partial h}{\partial x}) + \frac{\partial}{\partial y} (K_y (\frac{\partial h}{\partial y} + B)) + n\beta_T \frac{\partial T}{\partial t} + m_v = S_s \frac{\partial h}{\partial t} \quad (1)$$

where

$$h = \frac{p}{\rho^*g} + y - y^* \quad (2)$$

is the hydraulic head at a reference fluid density

$$B = (\rho/\rho^*) - 1 \quad (3)$$

is the buoyancy gradient created by density variations due to nonisothermal conditions in the flow field, and where

- g = acceleration due to gravity (Lt^{-2})
- K_x = x-direction principle hydraulic conductivity (Lt^{-1})
- K_y = y-direction principle hydraulic conductivity (Lt^{-1})
- m_v = fluid source/sink term (t^{-1})

- n = porosity (dimensionless)
 p = thermodynamic pressure ($ML^{-1}t^{-2}$)
 r = radial coordinate (L), $r \rightarrow \infty$ if cartesian coordinates are used
 S_s = specific storage (L^{-1})
 T = fluid-medium temperature
 t = time
 x, y = cartesian space coordinates (L)
 y^* = reference datum for y-coordinate (L)
 β_T = temperature compressibility of fluid (T^{-1})
 ρ = actual fluid density (ML^{-3})
 ρ^* = reference fluid density (ML^{-3}).

In addition to the governing equation (Eq. 1), initial and boundary conditions are specified to provide a complete description of the hydraulic head field. The initial condition is specified as

$$h(x, y, t') = f(x, y) \quad (4)$$

where

$t' < t$ = the time at which the head field is fully known. Generally t' is taken to be zero.

The general form of the boundary condition is

$$K_n \left(\frac{\partial h}{\partial n} \right) + a(x, y, t)h = b(x, y, t) \quad (5)$$

where

n = a direction normal to the boundary.

When $a \rightarrow \infty$ and $b = a \cdot h_b$, where h_b is the specified head, Equation 5 represents the Dirichlet boundary; it represents the Neumann boundary, if $a = 0$ and $b = Q$ where Q is the flux per unit area normal to the boundary. For arbitrary a and b , Equation 5 represents a mixed (Fourier) boundary condition.

3.2 GOVERNING EQUATIONS FOR TEMPERATURE AND MASS TRANSPORT

The governing equations for temperature and mass transport in PORSTAT are exactly the same as in PORFLO. Their numerical treatment also remains unchanged. The details of these equations are available elsewhere (Runchel, 1982; Runchel and Hocking, 1981) and will not be discussed in this report.

3.3 DISCRETIZATION OF THE GROUNDWATER FLOW EQUATION

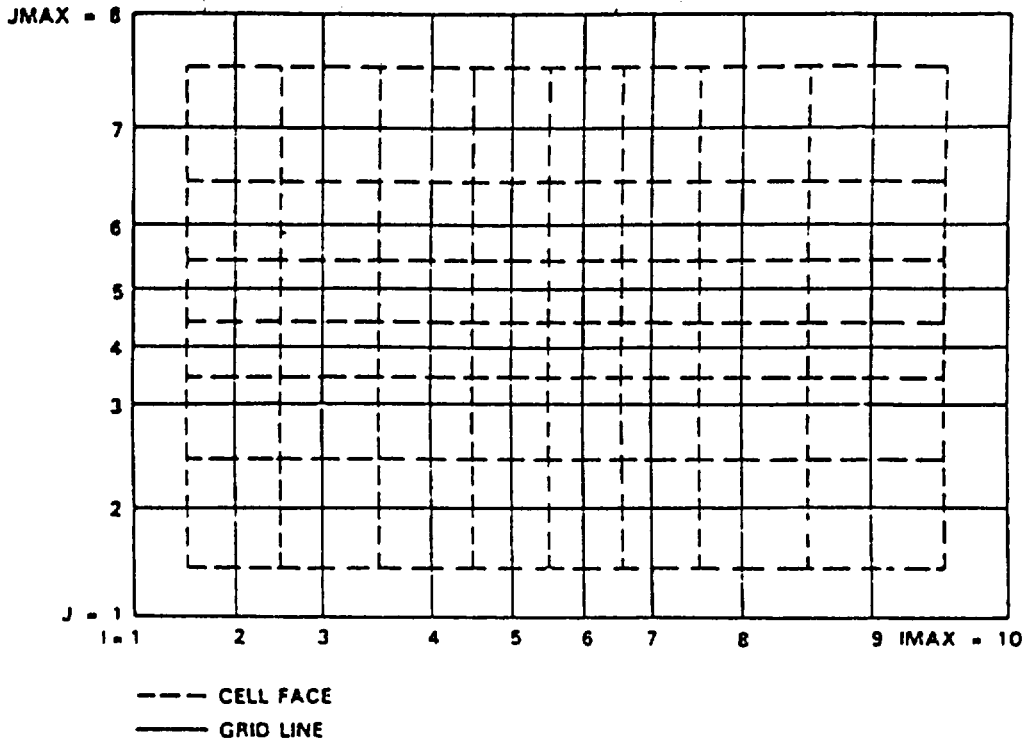
3.3.1 The Grid: The Point Centered Grid System

A point-centered grid system (Peaceman, 1977, p. 39) as shown in Figure 2 is used in PORSTAT for the numerical solution. In this system, the nodes lie at the intersections of the grid lines, which may or may not be uniformly spaced. Cell interfaces are drawn exactly midway between the grid lines. Thus each node has a cell associated with it. Note, however, that the nodes are not in the middle of the cells unless the grid lines are uniformly spaced. In the solution algorithm followed in PORSTAT, fluxes and velocities are calculated at the cell faces and state variables such as hydraulic head, temperatures, and concentrations are calculated at the nodes. From here on, it is assumed that the vertical grid lines are numbered as $I = 1, 2, \dots, I_{MAX}$ and the horizontal as $J = 1, 2, \dots, J_{MAX}$.

3.3.2 Discretization: Method of Nodal Point Integration

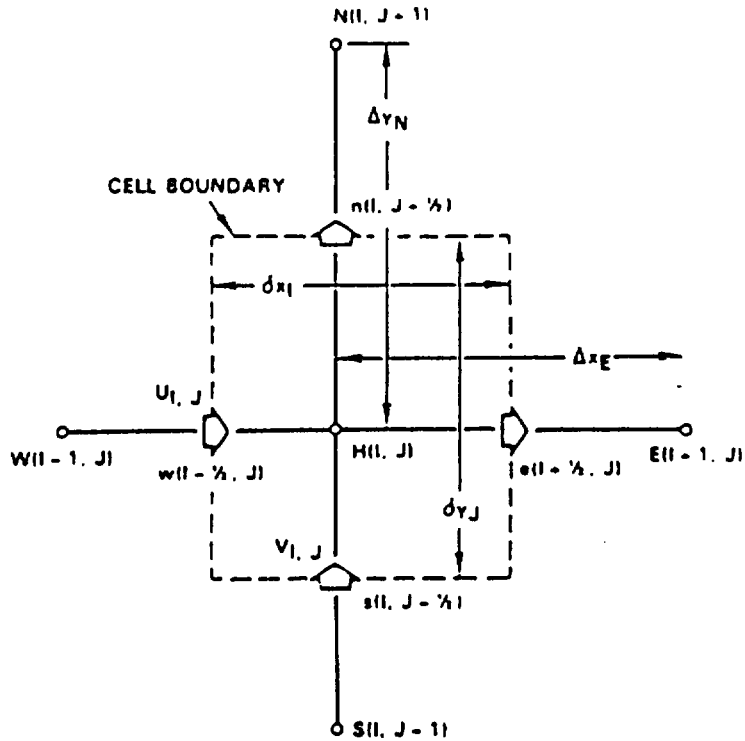
The method of nodal point integration is used to discretize Equation 1. A typical cell of the numerical grid associated with grid node labeled as $H(I, J)$ is shown in Figure 3. The nodes labeled as $E(I+1, J)$, $W(I-1, J)$, $N(I, J+1)$, and $S(I, J-1)$ are located to the immediate east, west, north, and south of $H(I, J)$. Points $e(I+1/2, J)$, $w(I-1/2, J)$, $n(I, J+1/2)$, and $s(I, J-1/2)$ are on cell faces where velocities and fluxes are computed. The discretized form of Equation 1 for node $H(I, J)$ is obtained by integrating it over its associated grid cell (from w to e and s to n) and over the time interval N to $N+1$. For the groundwater flow equation, second-order profiles are assumed between w and e as well as between s and n (for more details see Patankar, 1981). The discretized equation so obtained is

$$\begin{aligned}
 A(I+1/2, J, N) h(I+1, J, N+1) &+ A(I-1/2, J, N) h(I-1, J, N+1) \\
 &+ A(I, J+1/2, N) h(I, J+1, N+1) \\
 &+ A(I, J-1/2, N+1) h(I, J-1, N+1) \\
 &+ A(I, J, N) h(I, J, N+1) = R(I, J) \quad (6)
 \end{aligned}$$



PS8307-19

FIGURE 2. Example of Point Centered Grid System.



PS8307-20

FIGURE 3. A Typical Grid Cell.

Note that all hydraulic heads are written at time $N+1$, and, hence, the equation is fully implicit. The coefficients A are given as follows:

$$A(I+1/2, J, N) = -r_e K_x(I+1/2, J, N) \frac{y(J+1/2) - y(J-1/2)}{x(I+1) - x(I)} \quad (7)$$

$$A(I-1/2, J, N) = -r_w K_x(I-1/2, J, N) \frac{y(J+1/2) - y(J-1/2)}{x(I) - x(I-1)} \quad (8)$$

$$A(I, J+1/2, N) = -K_y(I, J+1/2, N) \frac{x(I+1/2) - x(I-1/2)}{y(J+1) - y(J)} \quad (9)$$

$$A(I, J-1/2, N) = -K_y(I, J-1/2, N) \frac{x(I+1/2) - x(I-1/2)}{y(J) - y(J-1)} \quad (10)$$

$$\begin{aligned} A(I, J, N) = & S_s(I, J) v(I, J) 1/[t(N+1)-t(N)] - A(I+1/2, J, N) \\ & - A(I-1/2, J, N) - A(I, J+1/2, N) - A(I, J-1/2, N) \end{aligned} \quad (11)$$

The $R(I, J)$ on the right of Equation 6 is given by

$$\begin{aligned} R(I, J) = & S_s(I, J) v(I, J) 1/[t(N+1)-t(N)] h(I, J, N) \\ & + B(I, J+1/2, N) - B(I, J-1/2, N) + m_v v(I, J) \\ & + m_T(I, J) v(I, J) \end{aligned} \quad (12)$$

where

$$v(I, J) = [x(I+1/2) - x(I-1/2)] \cdot [y(J+1/2) - y(J-1/2)] \quad (13)$$

is the volume of the cell and $m_T(I, J)$ is the term obtained from the $\partial T/\partial t$ term in Equation 1.

3.3.3 Incorporation of Boundary Conditions

Dirichlet and Neumann boundary conditions are considered in PORSTAT. These boundary conditions are incorporated into the numerical equations for nodes located next to the boundary. For example, consider nodes (2,J). These nodes are located next to the line of western boundary nodes (1,J). If the Dirichlet condition is given at (1,J), then

$$h(1,J,N+1) = h_B(1,J,N+1) \quad (14)$$

where

h_B = the specified boundary hydraulic head and is, therefore, a known quantity in the equation for node (2,J).

To account for this, the term $A(1,J,N+1) h_B(1,J,N+1)$ is transferred to the right-hand side of Equation 6, leaving only four unknown heads in the equation.

If the hydraulic head is specified at the cell face, then

$$h(1,J,N+1) = 2h_B(1+1/2,J,N+1) - h(2,J,N+1) \quad (15)$$

and the coefficient $A(2,J,N+1)$ and the right-hand side are both modified. Finally for the Neumann condition

$$h(1,J,N+1) = \frac{Q(1,J,N+1) [x(2) - x(1)]}{K_x(1+1/2,J,N)} + h(2,J,N+1) \quad (16)$$

where

$Q(1,J,N+1)$ = the specified flux per unit cross-sectional area.

Again through the use of Equation 16, $h(1,J,N+1)$ is eliminated from the equation pertaining to node (2,J).

3.3.4 Formation of Random Equations

In this study, some or all of the hydraulic conductivities, specific storages, boundary conditions, and initial conditions can be stochastic quantities. Under such conditions, Equation 1 and its numerical approximation, Equations 6 to 16, become random equations. It is this set of random algebraic equations that is solved in PORSTAT by the second-order method, the theory of which is described below.

3.4 THEORY OF SECOND-ORDER ANALYSIS

3.4.1 Concept of Solution of Random Algebraic Equations

The set of random algebraic equations obtained by discretizing the random differential Equation 1 may be written in a concise form as

$$[A]\{h\} = \{R\} \quad (17)$$

where

$[A]$ = the matrix whose elements are the coefficients $A(L,M)$ of Equations 7 to 11

$\{h\}$ = the vector of hydraulic heads to be evaluated

$\{R\}$ = the vector of right-hand elements from Equation 12.

Since one equation is obtained for each interior node, the size of $[A]$ is equal to $\text{NOE} \times \text{NOE}$, where NOE = number of equations = $(\text{IMAX}-2) \times (\text{JMAX}-2)$. Because of randomness in the parameters, all or some of the elements of $[A]$ and $\{R\}$ are random variables so that the solution of Equation 17 (i.e., $\{h\}$) is also random. The complete solution of Equation 17 consists of determining all the finite-dimensional joint probability distribution functions of the random function $\{h\}$. If the joint probability distribution functions of all the elements of $[A]$ and $\{R\}$ are specified, then it is theoretically possible (e.g., Papoulis, 1965) to determine the joint probability distribution functions of $\{h\}$. However, because of the very large number of the elements involved, it is not practicable to do so. For the purpose of this study, estimates of the mean and covariance of $\{h\}$ are deemed to constitute a solution of Equation 17.

3.4.2 Principal of Second-Order Analysis

The second-order method is based on the principle of expanding the vector $\{h\}$ by a Taylor series in terms of the parameters about their expected values. The parameters that are considered to be uncertain in this study are the hydraulic conductivities, K_x and K_y ; the specific storage, S_s ; the boundary conditions on the west (WBC), east (EBC), south (SBC), and north (NBC); and the initial condition, h^0 . The expected values and the covariance matrices of all the stochastic quantities are to be specified at appropriate locations on the grid defined in Section 3.3.1. For example, the moments of K_x are specified at $(I+1/2, J)$, those of K_y at $(I, J+1/2)$, WBC at $(1, J)$, EBC at (IMAX, J) , SBC at $(I, 1)$, NBC at (I, JMAX) , and h^0 at all remaining nodes. Note that each element h_m of $\{h\}$ is a function of all the uncertain parameters at all locations. For economy of writing the next few equations, denote

the uncertain parameters by a_i , $i=1,2,\dots,M$, where M is the total number of random variables of which h_m is a function, so that

$$h_m = f_m(a_i) \quad (18)$$

Expanding h_m in a Taylor series, results in

$$\begin{aligned} h_m &= f_m(\bar{a}_i) + \sum_i (a_i - \bar{a}_i) (\partial f_m / \partial a_i) \\ &+ \sum_i (1/2) (a_i - \bar{a}_i)^2 (\partial^2 f_m / \partial a_i^2) \\ &+ \sum_i \sum_{\substack{j \\ i > j}} (a_i - \bar{a}_i)(a_j - \bar{a}_j) (\partial^2 f_m / \partial a_i \partial a_j) + \dots \end{aligned} \quad (19)$$

where a bar over a variable represents its expected value and the derivatives are to be evaluated at the expected values. Note that these derivatives are in fact the sensitivity coefficients. The mean of h_m can now be easily written down as

$$\begin{aligned} \bar{h}_m &= f_m(\bar{a}_i) + \frac{1}{2} \sum_i \text{Var } a_i \cdot (\partial^2 f_m / \partial a_i^2) \\ &+ \sum_i \sum_{\substack{j \\ i > j}} \text{Cov } a_i, a_j \cdot (\partial^2 f_m / \partial a_i \partial a_j) \end{aligned} \quad (20)$$

where Var and Cov are respectively the variance and covariance of the random variables. It is interesting to note that in a first-order analysis, the second-order derivatives are neglected, in which case,

$$h_m = f_m(\bar{a}_i) \quad (21)$$

i.e., the expected value is the same as would be obtained if the deterministic problem is solved using the expected values of the parameters. In the second-order analysis, however, due to the nonlinearity of f , extra terms appear.

The covariance of (h_m, h_n) can similarly be obtained as

$$\begin{aligned} \text{Cov}(h_m, h_n) &= \sum_i \text{Var}[a_i] (\partial f_m / \partial a_i) (\partial f_n / \partial a_i) \\ &+ \sum_i \sum_{j > i} \text{Cov}[a_i, a_j] (\partial f_m / \partial a_i) (\partial f_n / \partial a_j) \end{aligned} \quad (22)$$

Note that the function f_m or f_n is defined by Equation 17. Since in Equations 20 and 22, the evaluation of the vector $\{f\}$ and its derivatives is at expected values of the random parameters, $\{f\}$ is simply

$$\{f\} = [A^0]^{-1} = \{D\} \quad (23)$$

where

$[A^0]$ = the matrix $[A]$ with its random elements assuming their expected values.

As would be evident from the following section, explicit evaluation of $\{D\}$ would be required for the implementation of the second-order analysis.

3.5 EVALUATION OF FIRST- AND SECOND-ORDER DERIVATIVES

For the application of Equations 20 and 22, first- and second-order derivatives of $\{f\}$ with respect to a_i are needed. In matrix theory (Faddeev and Faddeeva, 1963, p. 123), it is known that

$$\partial D(M,N) / \partial A(K,L) = -D(M,K)D(L,N). \quad (24)$$

In PORSTAT, the two-dimensional array of hydraulic heads $h(I,J)$ is mapped into a one-dimensional array by numbering the nodes sequentially in a columnar fashion; i.e., $h(2,2)$, $h(2,3)$, ..., $h(3,2)$, $h(3,3)$, ... are mapped into $h(1)$, $h(2)$, ... etc., such that $h(I,J)$ may be written as

$$h(I,J) = h(M) = \sum_M D(M,L)R(M). \quad (25)$$

Thus the M th unknown hydraulic head is a function of the M th row of $\{D\}$ and the entire vector $\{R\}$. The equations for the first- and second-order derivatives of $\{h\}$ with respect to the uncertain parameters can be derived based

on Equations 24 and 25 and from knowledge of the structure of the matrix [D]. A brief derivation of these equations is presented in Appendices A and B, respectively.

It should be noted that the first-order derivatives are also called the sensitivity coefficients. Thus, the entire array of sensitivity coefficients (i.e., the sensitivity of hydraulic head at each internal node with respect to all the uncertain parameters at all the nodes) is explicitly calculated as an intermediate step in PORSTAT.

3.6 EXPECTED VALUE AND COVARIANCE OF DARCIAN VELOCITY

The Darcian velocities, U in the x- and V in the y-coordinate direction, are given by

$$U(I+1/2, J, N) = K_x(I+1/2, J, N) \frac{h(I, J, N) - h(I+1, J, N)}{x(I+1/2) - x(I-1/2)} \quad (26)$$

$$V(I, J+1/2, N) = K_y(I, J+1/2, N) \frac{h(I, J, N) - h(I, J+1, N)}{y(J+1/2) - y(J-1/2)} \quad (27)$$

While developing equations for the expected value and covariance of U and V, it should be noted that not only are the hydraulic head h and the hydraulic conductivity K_x and K_y stochastic variables, but they are also correlated with each other. In addition, since U and V are functions of h, and since h at each node is a function of all the uncertain parameters at all nodes, U and V are in effect, functions of all the uncertain parameters. Keeping this in mind, equations similar to Equation 17 may be written for U and V and their expected values and variances obtained. The derivation of these equations is provided in Appendix C.

3.7 SUMMARY AND DISCUSSION

The basic assumption in computing the expected value of the hydraulic head is that the Taylor expansion containing terms of up to second order is an adequate representation of the head in the parameter space. Note that the expansion is in terms of the parameters and not in terms of the space coordinates. This expansion would be exact if derivatives of hydraulic head with respect to parameters of order higher than two were zero. Although Equation 1 itself has not been solved analytically, a number of analytic solutions of its simpler analogues are available in literature. From these solutions, it is apparent that the solution is of the exponential type with the parameters occurring in the exponent. The exponent is, in general, of the type $-Sx^2/4Kt$. Thus derivatives of all orders with respect to hydraulic conductivity and storativity exist and can be nonzero. However, it is also apparent that as the order of the derivatives increases, their magnitude decreases. Neglecting derivatives of order higher than two, therefore, is not inconsistent with the physical nature of the problem.

It should be noted that the solution of Equation 1 is a linear function of the initial and boundary conditions. The effect of uncertainties in these two parameters, therefore, is represented exactly in the second-order analysis.

Additional terms are neglected in writing Equation 22 for the covariance of pressure. In arriving at this equation, not only the terms that contain derivatives of third or higher order but also terms containing statistical moments of order greater than two are neglected. Inclusion of higher-order terms would require specification of higher-order moments, which are often not available in the field and even if available, their inclusion would increase the computational burden considerably.

4.0 APPLICATION OF PORSTAT TO TEST CASES

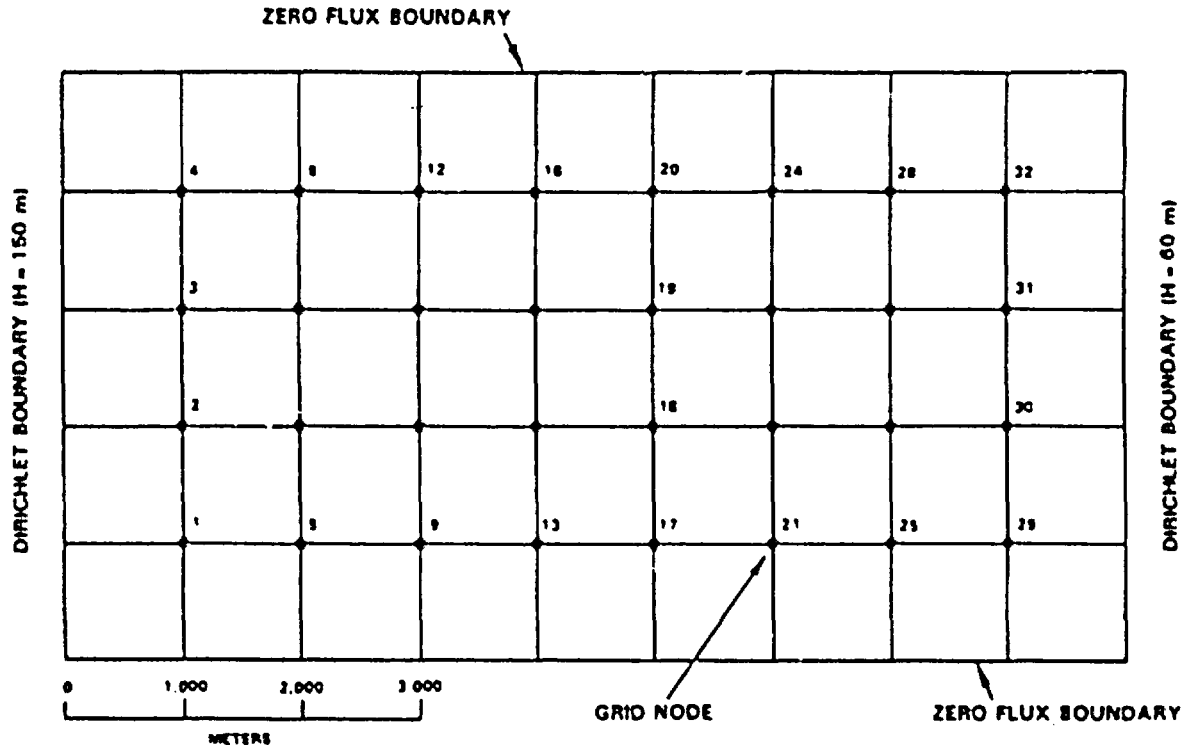
This section describes the application of PORSTAT to two simple test cases. These test cases were designed to provide initial evaluation of the ability of PORSTAT to solve the stochastic groundwater flow equation. In order to make this confirmation, the results from PORSTAT are compared with Monte Carlo analyses of the same two test cases. The Monte Carlo analyses were carried out by Rockwell using the deterministic computer code MAGNUM (Baca et al., 1983). For convenience, the Monte Carlo version of MAGNUM is called MAGNUM-MC. The mechanics of the Monte Carlo analysis method are described in Appendix D.

4.1 TEST CASE 1

4.1.1 Physical Description and Grid System

This test case involved solving for the steady-state hydraulic head field in a rectangular domain 9,000 by 5,000 m. The hydraulic conductivity field in this domain was homogenous and isotropic, and also stochastic. Boundary conditions were deterministically set. The hydraulic gradient in the x-direction was -0.01, and in the y-direction was zero.

The grid system and boundary conditions used by PORSTAT to solve the first test case is shown in Figure 4. For brevity, only the internal nodes of the grid are numbered because these will be the only nodes used to compare results from PORSTAT and MAGNUM-MC. The grid and boundary conditions used by MAGNUM-MC to solve the same test case by means of the Monte Carlo technique are the same as shown in Figure 4. MAGNUM uses a finite-element numerical scheme and requires isoparametric rectangular or triangular elements (Baca et al., 1983). In this case, eight-noded rectangular elements were used. The grid systems for PORSTAT and MAGNUM-MC were designed so that there would be a direct correspondence between the nodes of each grid.



PS8307-21

FIGURE 4. Grid System and Boundary Conditions Input to PORSTAT, Test Case 1.

4.1.2 Stochastic Hydraulic Conductivity Data

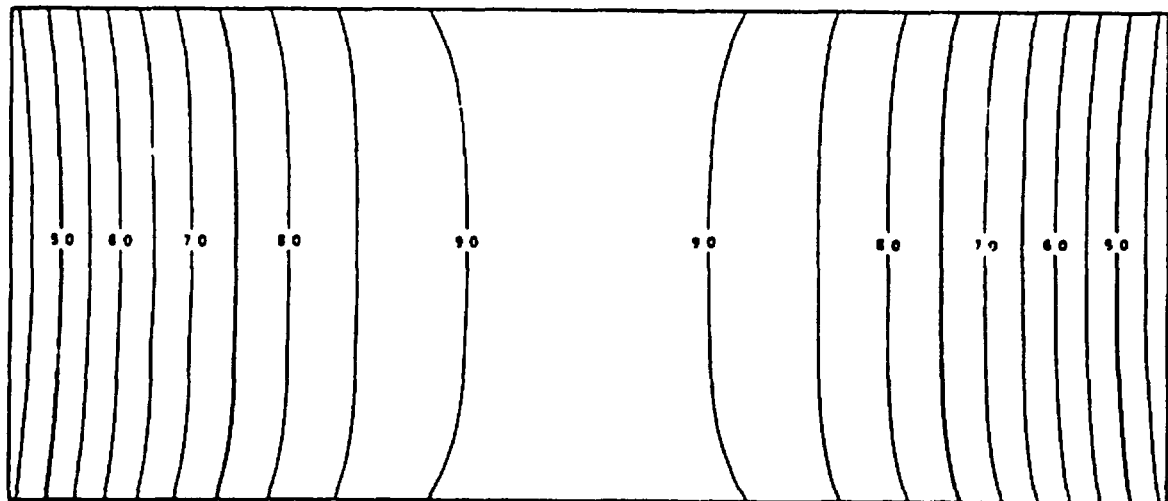
The stochastic input required by PORSTAT consisted of the expected values and the composite covariance matrix of the x- and y-direction hydraulic conductivities. The expected values of hydraulic conductivity were uniformly set at 38.1 m/yr. The composite covariance matrix of hydraulic conductivity and the method used to generate this matrix are described in Appendix E. The diagonal elements of this matrix (i.e., the variances) were uniformly set at 671.4 (m/yr)². The covariances between hydraulic conductivities were determined from a smoothly decreasing correlation function that had twice the range of correlation in the x-direction than in the y-direction.

The stochastic input required by MAGNUM-MC consisted of a suite of random hydraulic conductivity fields having the same covariance structure as the hydraulic conductivity field used by PORSTAT. Appendix E describes the method of developing the suite of random hydraulic conductivity fields.

4.1.3 Results

The deterministic hydraulic head field within the modeled domain uniformly decreases between the two constant head boundaries because of the homogeneous hydraulic conductivity field. However, the expected values of hydraulic head computed by PORSTAT differ slightly from the deterministic heads because of the formulation of the second-order uncertainty analysis method (see Eq. 20). The deterministic hydraulic head solution and the expected values of hydraulic head calculated by PORSTAT and MAGNUM-MC are compared in Table 1. As can be seen from this table, the absolute difference between the deterministic solution and both stochastic solutions, and between the stochastic solutions, is negligible in comparison with the total head drop across the modeled domain.

The standard deviations of hydraulic head determined by PORSTAT are contoured in Figure 5. These standard deviations tend to increase toward the center of the domain away from the two constant head boundaries. The marked effect the constant head boundaries have on the magnitude of the standard deviations is readily apparent. The symmetry of the standard deviation field is a consequence of the symmetric nature of the correlation structure of the hydraulic conductivity field. Curiously, the hydraulic head standard deviation tends to be larger near the two zero flux boundaries. It is not as yet clear what causes this magnification of the uncertainty in hydraulic head near these boundaries.



STANDARD DEVIATIONS OF HYDRAULIC HEAD ARE IN METERS

PS8307 22

FIGURE 5. Standard Deviation of Hydraulic Head Computed by PORSTAT, Test Case 1.

TABLE 1. Deterministic Solution and Expected Values of Hydraulic Head, Test Case 1.

Node	Deterministic solution	Expected value		Differences		
		PORSTAT	MAGNUM-MC	PORSTAT-deterministic solution	MAGNUM-MC-deterministic solution	MAGNUM-MC-PORSTAT
1	140.000	140.007	140.010	0.007	0.010	0.003
2	140.000	140.001	139.990	0.001	-0.010	-0.011
3	140.000	140.001	139.810	0.001	-0.190	-0.191
4	140.000	140.007	139.770	0.007	-0.230	-0.237
5	130.000	130.067	130.130	0.067	0.130	0.063
6	130.000	130.042	130.070	0.042	0.070	0.028
7	130.000	130.042	130.000	0.042	0.000	-0.042
8	130.000	130.067	130.070	0.067	0.070	0.003
9	120.000	120.062	120.360	0.062	0.360	0.298
10	120.000	120.044	120.360	0.044	0.360	0.316
11	120.000	120.044	120.500	0.044	0.500	0.456
12	120.000	120.062	120.710	0.062	0.710	0.648
13	110.000	110.023	110.490	0.023	0.490	0.467
14	110.000	110.018	110.540	0.018	0.540	0.522
15	110.000	110.018	110.610	0.018	0.610	0.592
16	110.000	110.023	110.490	0.023	0.490	0.467
17	100.000	99.978	100.610	-0.022	0.610	0.632
18	100.000	99.983	100.630	-0.017	0.630	0.647
19	100.000	99.983	100.590	-0.017	0.590	0.607
20	100.000	99.978	100.360	-0.022	0.360	0.382
21	90.000	89.939	90.580	-0.061	0.580	0.641
22	90.000	89.956	90.430	-0.044	0.430	0.474
23	90.000	89.956	90.410	-0.044	0.410	0.454
24	90.000	89.939	90.320	-0.061	0.320	0.381
25	80.000	79.933	80.520	-0.067	0.520	0.587
26	80.000	79.959	80.200	-0.041	0.200	0.241
27	80.000	79.959	80.190	-0.041	0.190	0.231
28	80.000	79.933	80.290	-0.067	0.290	0.357
29	70.000	69.993	70.220	-0.007	0.220	0.227
30	70.000	69.999	70.080	-0.001	0.080	0.081
31	70.000	69.999	70.090	-0.001	0.090	0.091
32	70.000	69.993	70.190	-0.007	0.190	0.197

The hydraulic head standard deviations computed by PORSTAT and those computed by MAGNUM-MC are compared in Table 2. It is apparent that the standard deviations computed by PORSTAT are consistently higher than the standard deviations computed by MAGNUM-MC. The maximum difference between the two sets of standard deviations is ~22%. Assuming that the Monte Carlo analysis by MAGNUM-MC is more accurate because effectively moments of all orders were considered, it is apparent that PORSTAT in this test case produced conservative results from the view of risk analysis.

TABLE 2. Standard Deviation of Hydraulic Head,
Test Case 1.

Node	Standard deviation		Percent difference $100(\text{PORSTAT}-\text{MAGNUM-MC})/\text{MAGNUM-MC}$
	PORSTAT	MAGNUM-MC	
1	4.326	3.659	17.08
2	4.099	3.548	15.53
3	4.099	3.680	11.39
4	3.326	3.800	13.84
5	6.988	5.994	16.58
6	6.795	6.051	12.30
7	6.795	6.069	11.96
8	6.988	6.153	13.57
9	8.526	7.384	15.47
10	8.392	7.497	11.94
11	8.392	7.632	9.96
12	8.526	7.663	11.26
13	9.211	8.060	14.28
14	9.103	8.075	12.73
15	9.103	8.212	10.85
16	9.211	8.481	8.61
17	9.211	8.074	14.08
18	9.103	7.928	14.82
19	9.103	7.748	17.49
20	9.211	7.897	16.64
21	8.826	7.547	16.95
22	8.392	7.203	16.51
23	8.392	7.078	18.56
24	8.826	7.220	22.24
25	6.988	6.069	15.14
26	6.795	5.768	17.81
27	6.795	5.694	19.34
28	6.988	5.966	17.13
29	4.326	3.659	18.23
30	4.099	3.456	18.61
31	4.099	3.499	17.15
32	4.326	3.712	16.54

Figures 6 and 7 illustrate the correlation structure of hydraulic head along four cross sections through the modeled domain. Results from both PORSTAT and MAGNUM-MC are presented. It is apparent that the hydraulic head correlation structures predicted by PORSTAT and MAGNUM-MC are very similar. Also evident is the slightly stronger correlation in the y-direction in Figure 7. This is most likely caused by the boundary conditions assigned to the model domain, which prevents groundwater flow in the y-direction.

4.2 TEST CASE 2

4.2.1 Physical Description and Grid System

The same model domain and boundary conditions used in Test Case 1 (Fig. 4) were also used in the second test case. However, the hydraulic conductivity field in Test Case 2 was specified to be heterogeneous and isotropic, with a nonuniform covariance structure.

4.2.2 Stochastic Hydraulic Conductivity Data

Figure 8 is a contour map of the expected values of the hydraulic conductivity field input to PORSTAT in Test Case 2. Appendix F describes the method used to generate this distribution of hydraulic conductivities. The method used to generate the composite covariance matrix of the x- and y-direction hydraulic conductivities is also explained in Appendix F. Figure 9 is a plot of the standard deviations of hydraulic conductivity input to PORSTAT. (The standard deviations are the square roots of the elements on the main diagonal of the composite covariance matrix.)

As in Test Case 1, the stochastic input required by MAGNUM-MC in the second test case consisted of a suite of random hydraulic conductivity fields having the same covariance structure as the hydraulic conductivity field input to PORSTAT. The method used to generate these fields is explained in Appendix F.

4.2.3 Results

In contrast to Test Case 1, the deterministic hydraulic head field is nonuniform within the model domain because of the heterogeneous hydraulic conductivity field. Figure 10 is a contour map of the deterministic head field. This head field was computed by arbitrarily setting to zero all the covariances between hydraulic conductivities input to PORSTAT. Slight differences exist between the deterministic solutions of PORSTAT and MAGNUM-MC. These differences are most likely due to the different numerical schemes used by each computer code and the slight differences between the hydraulic conductivity fields input to each code because of mesh geometry constraints. Appendix F explains these latter differences in more detail. Only the deterministic solution by PORSTAT is presented here so that a meaningful comparison can be made between this solution and the second-order solution calculated by PORSTAT using a nonzero hydraulic conductivity covariance matrix.

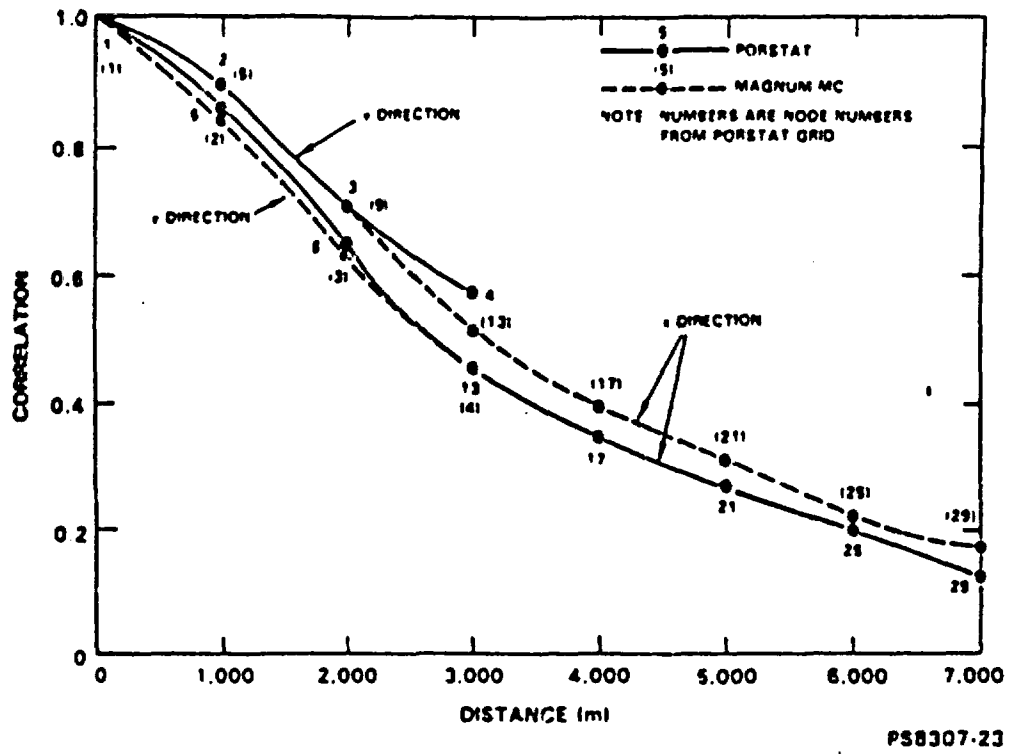


FIGURE 6. Hydraulic Head Correlation Structure From Node 1, Test Case 1.

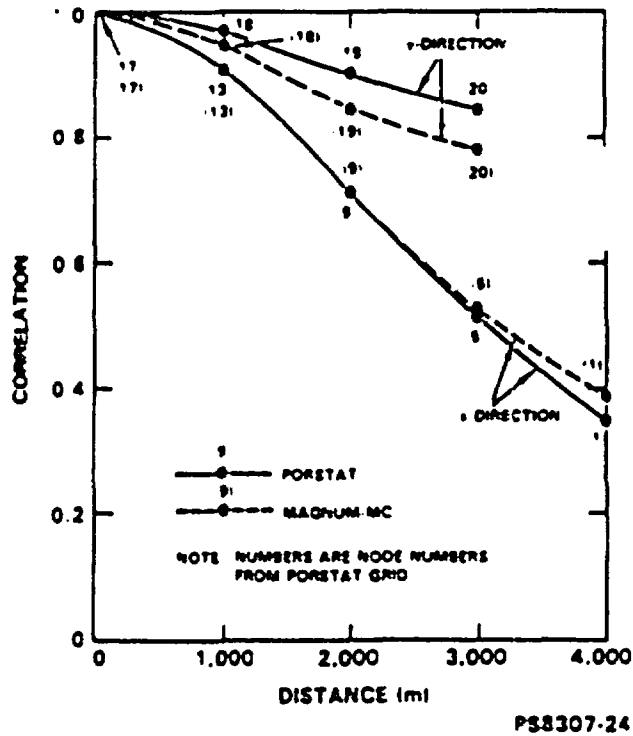
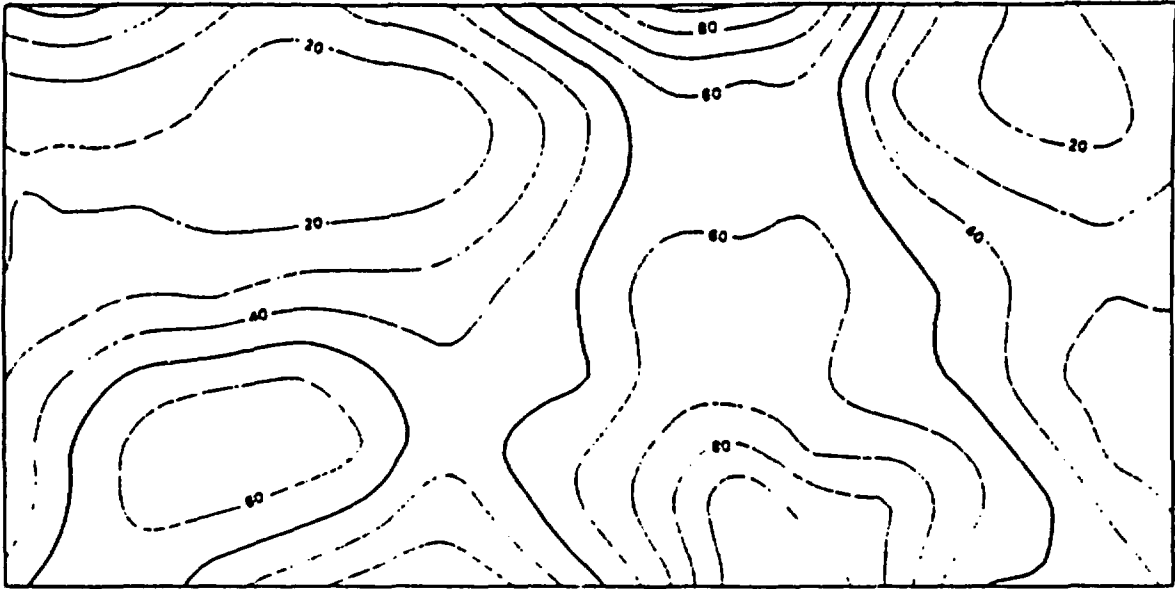


FIGURE 7. Hydraulic Head Correlation Structure From Node 17, Test Case 2.



EXPECTED VALUES OF HYDRAULIC CONDUCTIVITY ARE IN METERS PER YEAR

PS8307-25

FIGURE 8. Expected Values of Hydraulic Conductivity Input to PORSTAT, Test Case 2.



STANDARD DEVIATIONS OF HYDRAULIC CONDUCTIVITY ARE IN METERS PER YEAR

PS8307 26

FIGURE 9. Standard Deviation of Hydraulic Conductivity Input to PORSTAT, Test Case 2.

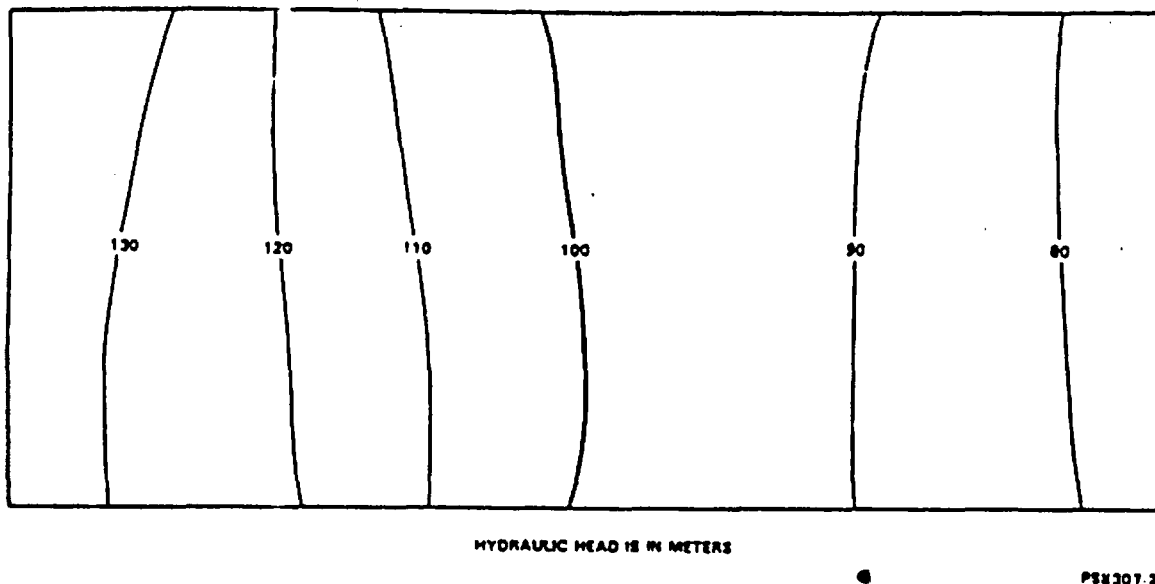


FIGURE 10. Deterministic Hydraulic Head Field Computed by PORSTAT, Test Case 2.

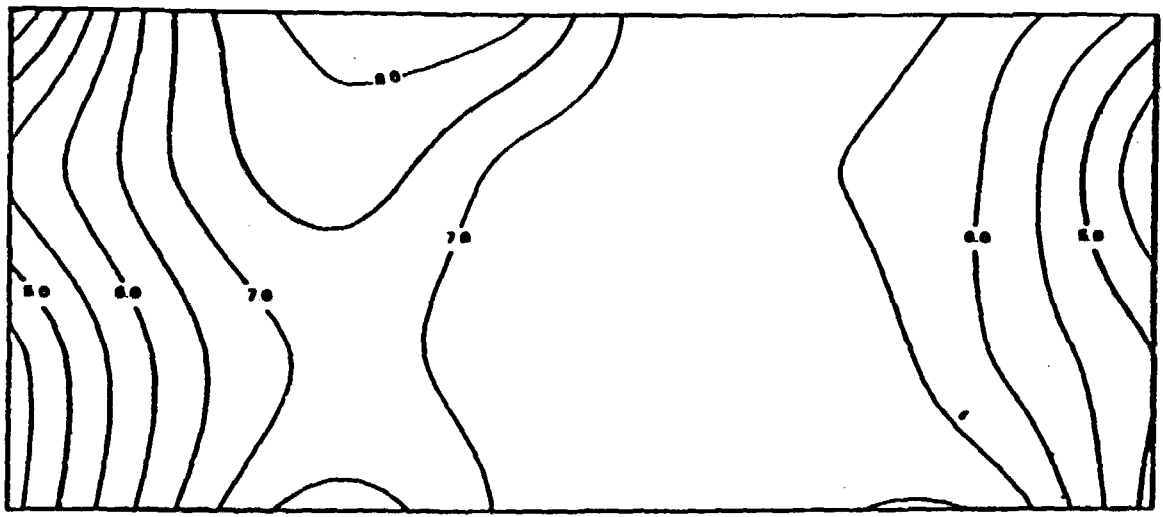
The deterministic hydraulic head field calculated by PORSTAT and the expected value of hydraulic head calculated by PORSTAT and MAGNUM-MC are compared in Table 3. The difference between the expected head field calculated by PORSTAT and the deterministic head field is significantly greater than the corresponding difference in Test Case 1. This indicates that the contribution from the second-order terms in Equation 20 is much greater in the second test case. The difference between the expected head fields calculated by PORSTAT and MAGNUM-MC are also greater than the corresponding difference in Test Case 1. All these differences are small, however, in comparison with the total head drop across the modeled domain.

Figure 11 is a contour map of the standard deviations of hydraulic head computed by PORSTAT. The nonuniformity of this standard deviation map is due to the heterogeneous nature and nonuniform covariance structure of the input hydraulic conductivity field. The standard deviations of hydraulic head computed by PORSTAT and MAGNUM-MC are compared in Table 4. At all but one node, the standard deviations computed by PORSTAT are greater than those computed by MAGNUM-MC. The maximum difference between standard deviations is 54%, and the average of the absolute values of the differences is 18%.

The correlation structures of hydraulic head determined by PORSTAT and MAGNUM-MC along four cross sections through the modeled domain are illustrated in Figures 12 and 13. The agreement between the correlation structures predicted by PORSTAT and MAGNUM-MC in this test case is not as close as the agreement in Test Case 1. Stronger correlation is apparent in the y-direction, and an explanation for this is given in the discussion of the results of Test Case 1.

TABLE 3. Deterministic Solution and Expected Values of Hydraulic Head, Test Case 2.

Node	Deterministic solution	Expected value		Differences		
		PORSTAT	MAGNUM-MC	PORSTAT-deterministic solution	MAGNUM-MC-deterministic solution	MAGNUM-MC-PORSTAT
1	135.258	137.562	139.540	2.304	4.282	1.978
2	135.521	136.780	138.350	1.259	2.829	1.570
3	137.858	137.909	139.470	0.051	1.612	1.561
4	139.780	141.492	142.450	1.712	2.670	0.958
5	126.738	126.440	129.440	-0.298	2.702	3.000
6	126.258	126.034	128.220	-0.224	1.962	2.186
7	127.241	126.139	128.770	-1.102	1.529	2.631
8	129.994	129.260	131.950	-0.734	1.956	2.690
9	117.560	116.240	118.680	-1.320	1.120	2.440
10	116.939	116.560	118.250	-0.379	1.311	1.690
11	115.000	115.391	117.410	0.391	2.410	2.019
12	113.331	115.633	118.010	2.302	4.679	2.377
13	104.013	104.189	105.840	0.176	1.827	1.651
14	104.654	105.227	106.060	0.573	1.406	0.833
15	102.997	104.710	105.400	1.713	2.403	0.690
16	101.572	107.008	105.880	5.436	4.308	-1.128
17	95.996	95.892	97.100	-0.104	1.104	1.208
18	96.385	95.926	97.290	-0.459	0.905	1.364
19	96.214	95.187	96.900	-1.027	0.686	1.713
20	95.936	95.552	97.740	-0.384	1.804	2.188
21	90.692	90.273	91.120	-0.419	0.428	0.847
22	90.745	90.107	91.450	-0.638	0.705	1.343
23	90.721	89.020	91.440	-1.701	0.719	2.420
24	91.367	87.658	91.510	-3.709	0.143	3.852
25	84.376	84.824	84.440	0.448	0.064	-0.384
26	83.983	83.625	84.440	-0.358	0.457	0.815
27	83.658	82.870	84.550	-0.788	0.892	1.680
28	84.305	82.403	84.570	-1.902	0.265	2.167
29	75.136	73.097	73.490	-2.039	-1.646	0.393
30	73.469	72.325	73.090	-1.144	-0.379	0.765
31	72.080	71.057	71.630	-1.023	-0.450	0.573
32	70.444	70.656	70.790	0.212	0.346	0.134



STANDARD DEVIATIONS OF HYDRAULIC HEAD ARE IN METERS

P82307-31

FIGURE 11. Standard Deviation of Hydraulic Head Computed by PORSTAT, Test Case 2.

TABLE 4. Standard Deviation of Hydraulic Head,
Test Case 2.

Node	Standard deviation		Percent difference $100(\text{PORSTAT}-\text{MAGNUM}-\text{MC})/\text{MAGNUM}-\text{MC}$
	PORSTAT	MAGNUM-MC	
1	4.267	3.179	34.22
2	4.376	3.685	18.75
3	5.571	3.628	53.56
4	3.971	3.373	17.73
5	6.482	5.810	11.57
6	6.241	5.521	13.04
7	6.991	5.496	27.20
8	7.052	5.976	18.01
9	7.764	6.219	24.84
10	7.097	5.864	21.03
11	7.764	6.087	27.55
12	8.243	7.414	11.18
13	6.980	5.780	20.76
14	6.781	5.605	20.98
15	6.856	5.728	19.69
16	8.235	6.946	18.56
17	6.880	5.829	18.03
18	6.654	5.787	14.98
19	6.594	5.717	15.34
20	6.689	6.181	8.22
21	6.930	5.928	16.90
22	6.804	5.931	14.72
23	6.517	5.807	12.23
24	6.829	6.213	9.91
25	6.897	6.064	13.74
26	5.970	5.127	16.44
27	5.922	5.135	15.33
28	6.228	5.925	5.11
29	4.784	3.619	32.19
30	4.961	4.286	15.75
31	4.064	4.480	-9.29
32	5.253	4.833	8.69

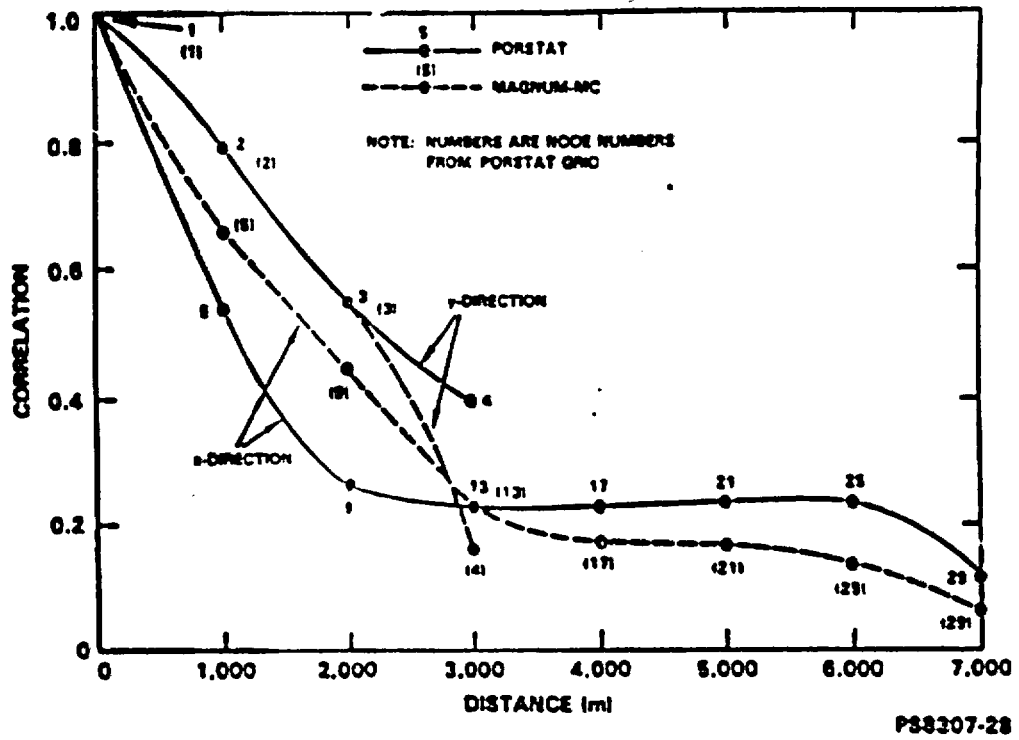


FIGURE 12. Hydraulic Head Correlation Structure From Node 1, Test Case 2.

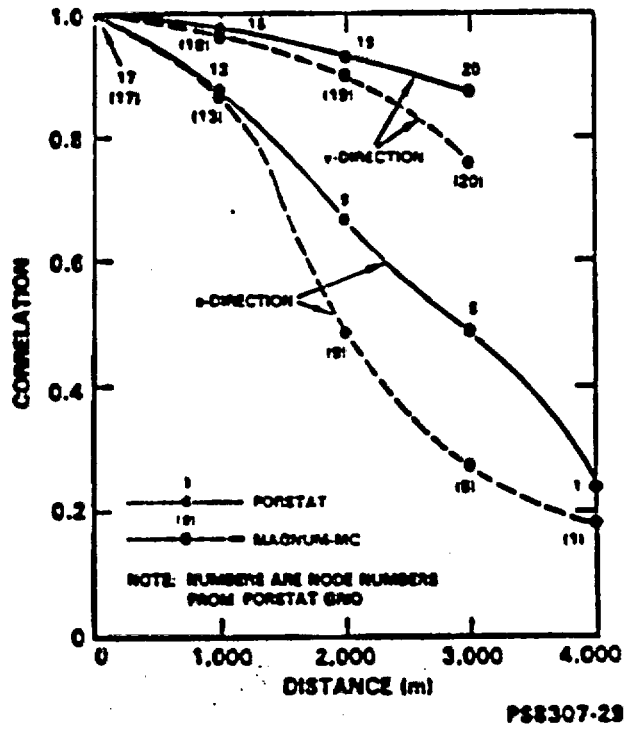


FIGURE 13. Hydraulic Head Correlation Structure From Node 17, Test Case 2.

5.0 SUMMARY AND CONCLUSIONS

This report documents the development and initial testing of the computer code PORSTAT. PORSTAT solves the stochastic groundwater flow equation coupled with the deterministic heat transfer and mass transport equations. Initial testing of PORSTAT was accomplished by cross checking the results of two simple test problems run by PORSTAT with the results of Monte Carlo analyses of these same two problems. The Monte Carlo analyses were completed by Rockwell using the computer code MAGNUM-MC.

PORSTAT solves the stochastic groundwater flow equation by means of the second-order uncertainty analysis technique. This technique is based on a second-order Taylor series expansion of hydraulic head about the expected values of the uncertain parameters after the governing equation has been numerically approximated by a series of linear algebraic equations. A major assumption in second-order uncertainty analysis is that the sum of third- and higher-order terms is negligible in comparison with the sum of the first- and second-order terms. The validity of this assumption is dependent on the type of groundwater flow problem being analyzed. For problems where the hydraulic head is a highly nonlinear function of hydraulic conductivity, this assumption may not be reasonable.

The major incentive for adopting the second-order uncertainty analysis technique is reduction in the computation time required to complete an uncertainty analysis. Ideally, Monte Carlo techniques provide the most reliable uncertainty analyses for complex problems involving a large number of uncertain parameters. This is because statistical moments of all orders are effectively considered in Monte Carlo analyses. However, a prohibitive amount of computer time would be needed if Monte Carlo techniques were used to analyze the coupled groundwater flow and heat transport problems currently being studied by Rockwell. For these problems, second-order uncertainty analysis offers a viable alternative to Monte Carlo techniques in terms of computation time.

The test cases analyzed in Section 4.0 were relatively simple steady-state groundwater flow problems. All inputs to both test cases were the same except for the hydraulic conductivity fields. In the first test case, the hydraulic conductivity field was homogeneous and isotropic and had a uniform covariance structure. In the second test case, the hydraulic conductivity field was heterogeneous and isotropic, with a nonuniform covariance structure.

The results from the test cases indicate that PORSTAT consistently predicted a higher standard deviation of hydraulic head than MAGNUM-MC except at one point in the model domain of the second test problem. The maximum differences between the standard deviations predicted by PORSTAT and MAGNUM-MC were 22% and 54% in the first and second test cases, respectively. Thus, from the point of view of risk analysis, PORSTAT, for the most part, produced conservative results in these test cases.

The results from the initial testing of PORSTAT indicate that the second-order uncertainty analysis method tends to overpredict the magnitude of the standard deviations of hydraulic head. The amount of overprediction is a function of the magnitude of the covariances of the uncertain parameters. As the covariances of the uncertain parameters becomes larger, the second-order method produces a poorer estimate of the uncertainties of the state variables of interest. Thus, prior to using PORSTAT for extensive estimation of uncertainties, it will be necessary to determine how much uncertainty can be tolerated in the parameters before the second-order method produces unacceptable results. These studies are being pursued by Rockwell.

6.0 REFERENCES

- Ahlstrom, S. W., Foote, H. P., Cole, R. C., and Serne, R. J., 1977, Multi-component Mass Transport Model: Theory and Numerical Implementation (Discrete Parcel Random Walk Version), BNWL-2127, Battelle, Pacific Northwest Laboratories, Richland, Washington.
- Arnett, R. C., Baca, R. G., Caggiano, J. A., Price, S. M., Gephart, R. E., and Logan, L. E., 1980, Preliminary Hydrologic Release Scenarios for a Candidate Repository Site in the Columbia River Basalts, RHO-BW1-ST-12, Rockwell Hanford Operations, Richland, Washington.
- Baca, R. G., Arnett, R. C., and Langford, D. W., 1983, Modeling Fluid Flow in Fractured-Porous Rock Masses by Finite-Element Techniques, RHO-BW-SA-297 P, Rockwell Hanford Operations, Richland, Washington.
- Bakr, A. A., Gelhar, L. W., Gutjahr, A. L., and Macmillan, J. R., 1978, "Stochastic Analysis of Spatial Variability in Subsurface Flows, 1: Comparison of One- and Three-Dimensional Flows," Water Resources Research, Vol. 14, No. 2, pp. 263-271.
- Clifton, P. M. and Neuman, S. P., 1982, "Effects of Kriging and Inverse Modeling on Conditional Simulation of the Avra Valley Aquifer in Southern Arizona," Water Resources Research, Vol. 18, No. 4, pp. 1215-1234.
- Deju, R. A., 1982, "Overview of the Basalt Waste Isolation Project," in Proceedings of the 1982 National Waste Terminal Storage Program Information Meeting, DOE/NWTS-30, Office of NWTS Integration, Columbus, Ohio, pp. 142-148.
- Dettinger, M. D. and Wilson, J. L., 1981, "First Order Analysis of Uncertainty in Numerical Models of Groundwater Flow, Part 1: Mathematical Development," Water Resources Research, Vol. 17, No. 1, pp. 149-161.
- Faddeev, D. K. and Faddeeva, V. N., 1963, Computational Methods of Linear Algebra, W. H. Freeman and Co., San Francisco, California.

- Freeze, R. A., 1975, "A Stochastic-Conceptual Analysis of One-Dimensional Groundwater Flow in Nonuniform Homogeneous Media," Water Resources Research, Vol. 11, No. 5, pp. 725-741.
- Gelhar, L. W., 1976, "Effect of Hydraulic Conductivity Variations on Groundwater Flows," in Proceedings of the 2nd International Symposium on Stochastic Hydraulics, International Association for Hydraulic Research, Lund, Sweden.
- Gephart, R. E., Arnett, R. C., Baca, R. G., Leonhart, L. S., and Spane, F. A. Jr., 1979, Hydrologic Studies Within the Columbia Plateau, Washington: An Integration of Current Knowledge, RHO-BWI-ST-5, Rockwell Hanford Operations, Richland, Washington.
- Gutjahr, A. L., Gelhar, L. W., Bakr, A. A., and Macmillan, J. R., 1978, "Stochastic Analysis of Spatial Variability in Subsurface Flows, 2: Evaluation and Applications," Water Resources Research, Vol. 14, No. 5, pp. 953-959.
- Harper, W. V., 1983, Sensitivity/Uncertainty Analysis for Nonstochastic Computer Codes, ONWI-444, Office of Nuclear Waste Isolation, Battelle Memorial Institute, Columbus, Ohio.
- Iman, R. L., Davenport, J. M. and Zeigler, D. K., 1980, Latin Hypercube Sampling (Program User's Guide), SAND79-1473, Sandia National Laboratories, Albuquerque, New Mexico.
- Journel, A. G. and Huijbregts, Ch. J., 1978, Mining Geostatistics, Academic Press, New York, New York.
- Kincaid, C. T., Vail, L. W., and Devary, J. L., 1983, Stochastic Ground Water Flow Analysis FY-81 Status, PNL-4025, Battelle, Pacific Northwest Laboratories, Richland, Washington.
- McLaughlin, D. B., 1979, Hanford Groundwater Modeling - Statistical Methods for Evaluating Uncertainty and Assessing Sampling Effectiveness, RHO-C-18, Rockwell Hanford Operations, Richland, Washington.
- Myers, C. W./Price, S. M., Caggiano, J. A., Cochran, M. P., Czimer, W. J., Davidson, H. J., Edwards, R. C., Fecht, K. R., Holmes, G. E., Jones, M. G., Kunk, J. R., Landon, R. D., Ledgerwood, R. K., Lillie, J. T., Long, P. E., Mitchell, T. H., Price, E. H., Reidel, S. P., and Tallman, A. M., 1979, Geologic Studies of the Columbia Plateau: A Status Report, RHO-BWI-ST-4, Rockwell Hanford Operations, Richland, Washington.
- Nuclear Waste Policy Act of 1982, Public Law 97-425.
- Oblow, E. M., 1978, "Sensitivity Theory for Reactor for Thermal-Hydraulics Problems," Nuclear Science and Engineering, Vol. 68, pp. 322-337.
- Oster, C. A., Gibbs, A. G., and Tang, D. H., 1981, "Analysis of a Numerical Solution to the One-Dimensional Stochastic Convection Equations," Advances in Water Resources, Vol. 4, pp. 2-8.

- Papoulis, A., 1965, Probability, Random Variables and Stochastic Processes, McGraw-Hill Book Co., New York, New York.
- Patankar, S. V., 1981, Numerical Heat Transfer and Fluid Flow, McGraw-Hill Book Co., New York, New York.
- Peaceman, D. W., 1977, Developments in Petroleum Science, Fundamentals of Numerical Reservoir Simulation, Series 6, Elsevier Scientific Publishing Co., New York, New York.
- Ripley, B. D., 1981, Spatial Statistics, John Wiley and Sons, Inc., New York, New York.
- Runchel, A. K., 1982, PORFLOW-R: A Mathematical Model for Coupled Groundwater Flow, Heat Transfer and Radionuclide Transport in Porous Media, ACRI/TN/006, Analytic and Computational Research, Inc., Los Angeles, California.
- Runchel, A. K., and Hocking, G., 1981, An Equivalent Continuum Model for Fluid Flow, Heat and Mass Transport in Geologic Materials, Paper 81-HT-54, Presented at the 20th Joint ASME/AIChE National Heat Transfer Conference, Milwaukee, Wisconsin, August 2-5, 1981.
- Rockwell, 1982, Site Characterization Report for the Basalt Waste Isolation Project, DOE/RL 82-3, Rockwell Hanford Operations, Richland, Washington.
- Sagar, B., 1978a, "Galerkin Finite Element Procedure for Analyzing Flow Through Random Media," Water Resources Research, Vol. 14, No. 6, pp. 1035-1044.
- Sagar, B., 1978b, "Analysis of Dynamic Aquifers with Stochastic Forcing Functions," Water Resources Research, Vol. 14, No. 2, pp. 207-216.
- Sagar, B., 1979, "Solution of Linearized Boussinesq Equation with Stochastic Boundaries and Recharge," Water Resources Research, Vol. 15, No. 3, pp. 618-624.
- Smith, L. and Freeze, R. A., 1979a, "Stochastic Analysis of Steady State Groundwater Flow in a Bounded Domain, 1: One-Dimensional Simulations," Water Resources Research, Vol. 15, No. 3, pp. 521-528.
- Smith, L. and Freeze, R. A., 1979b, "Stochastic Analysis of Steady State Groundwater Flow in a Bounded Domain, 2: Two-Dimensional Simulations," Water Resources Research, Vol. 15, No. 6, pp. 1543-1559.
- Smith, L. and Schwartz, F. W., 1980, "Mass Transport, 1: A Stochastic Analysis of Macroscopic Dispersion," Water Resources Research, Vol. 16, No. 2, pp. 303-313.
- Smith, L. and Schwartz, F. W., 1981a, "Mass Transport, 2: Analysis of Uncertainty in Prediction," Water Resources Research, Vol. 17, No. 2, pp. 351-369.

- Smith, L. and Schwartz, F. W., 1981b, "Mass Transport, 3: Role of Hydraulic Conductivity Data in Prediction," Water Resources Research, Vol. 17, No. 5, pp. 1463-1479.
- Spane, F. A., 1982, "Hydrologic Studies Within the Pasco Basin," in Proceedings of the 1982 National Waste Terminal Storage Program Information Meeting, DOE/NWTS-30, Office of NWTS Integration, Columbus, Ohio, pp. 23-28.
- Tang, D. H. and Pinder, G. F., 1977, "Simulation of Groundwater Flow and Mass Transport Under Uncertainty," Advances in Water Resources, Vol. 1, No. 1, pp. 25-30.
- Tang, D. H. and Pinder, G. F., 1979, "Analysis of Mass Transport with Uncertain Physical Parameters," Water Resources Research, Vol. 15, No. 5, pp. 1147-1155.
- Thomas, R. E., 1982, Uncertainty Analysis, ONWI-380, Office of Nuclear Waste Isolation, Battelle Memorial Institute, Columbus, Ohio.
- Warren, J. E. and Price, H. S., 1961, "Flow in Heterogeneous Porous Media," Society of Petroleum Engineers Journal, Vol. 1, pp. 153-169.

APPENDIX A

EQUATIONS FOR SENSITIVITY COEFFICIENTS

A.1 STRUCTURE OF COEFFICIENT MATRIX

The derivation of equations for the sensitivity coefficients (first-order derivatives) as well as for the second-order derivatives depends on the method of discretization used. In other words, an understanding of the structure of the coefficient matrix is necessary.

The matrix $[A]$, which is obtained after discretization of the governing equation, is banded, the bandwidth being dependent on the way the nodes are numbered. As pointed out in Section 3.5, the nodes are numbered in columnar manner in PORSTAT (i.e., nodes 1,2,... are respectively nodes (2,2), (2,3),... in the (I,J) system). $[A]$ is also symmetric and on each row, there are only five or less nonzero elements. It needs to be noted that each K_x and K_y of the internal nodes appear in two elements on one row of the matrix. For example, $K_x(I+1/2,J,N)$ appears in $A(I+1,J,N)$ and $A(I,J,N)$. Since the matrix is symmetric, in all, each K_x and K_y of internal nodes appear in a total of four elements of the matrix. None of these K_x and K_y appear on the right-hand side. For the nodes on the boundary, their K_x and K_y appear only in one--the main diagonal of the matrix, but they may appear on the right-hand side vector $\{R\}$.

Similarly, it is to be noted that, the specific storage appears only on the elements on the main diagonal of the matrix and on the right-hand side. The boundary conditions appear only on the right-hand side and only in equations for nodes adjacent to the boundaries. The initial condition (or the conditions at the previous time step) appear only on the right-hand side.

Knowing the structure of the matrix as above, helps in the computation of the sensitivity coefficients as explained below. In the following, it should be noted that, for notational convenience, $K_x(L,M)$ is written in place of $K_x(L-1/2,M,N)$. Similarly, the time index N is omitted from h also.

A.2 SENSITIVITY COEFFICIENT WITH RESPECT TO K_x

Consider the hydraulic head h at node (I,J) , $I=2,\dots, I_{MAX1}$ and $J=2,\dots, J_{MAX1}$, where $I_{MAX1}=I_{MAX}-1$ and $J_{MAX1}=J_{MAX}-1$. The first-order derivative $\partial h(I,J)/\partial K_x(L,M)$ may be written symbolically as

$$\begin{aligned} \frac{\partial h(I,J)}{\partial K_x(L,M)} &= \frac{\partial h(N)}{\partial K_x(L,M)} = \sum_M \frac{\partial D(N,k)}{\partial K_x(L,M)} R(M) \\ &+ \sum_M D(N,k) \frac{\partial R(M)}{\partial K_x(L,M)} \end{aligned} \quad (A-1)$$

where

$h(I,J)$ or $h(N)$ = the hydraulic head at node (I,J) or N, assuming nodes are numbered by column (see Fig. 4),
 $N = (I-2) \times \text{NOJ} + J-1$ where $\text{NOJ} = \text{JMAX}-2$

$K_x(L,M)$ = the x-direction hydraulic conductivity at node (L,M)

$D(N,k)$ = an element of the matrix D, which is inverse of the matrix $[A^0]$, formed by using expected values of the parameters

$R(M)$ = an element of the right-hand vector of the equation $[A] \{h\} = \{R\}$

NOE = the number of equations = number of internal nodes
 $= (\text{IMAX}-2) \times (\text{JMAX}-2)$.

The first term on the right-hand side of Equation A-1 is

$$\begin{aligned} \text{Term I} &= \frac{\partial D(N,k)}{\partial K_x(L,M)} R(M) \\ &= \sum_M \frac{\partial D(N,k)}{\partial A(I',J')} \frac{\partial A(I',J')}{\partial K_x(L,M)} R(M). \end{aligned} \quad (\text{A-2})$$

As explained in Section A.1, $K_x(L,M)$ is contained only in a limited number of $A(I',J')$. To recapitulate, the numerical scheme employed in PORSTAT has the following characteristics:

- For (L,M) not in the immediate vicinity of a boundary, $K_x(L,M)$ appears in four $A(I',J')$ s. There are $A(NL,NL)$, $A(NL,NK)$, $A(NK,NL)$, and $A(NK,NK)$, where, $NL = (L-3) \times \text{NOJ} + M-1$ and $NK = (L-2) \times \text{NOJ} + M-1$. Thus, the right-hand side of Equation A-2 is

$$\begin{aligned} \text{Term I} &= \sum_M \frac{\partial D(N,k)}{\partial A(NL,NL)} \frac{\partial A(NL,NL)}{\partial K_x(L,M)} R(M) \\ &+ \sum_M \frac{\partial D(N,k)}{\partial A(NL,NK)} \frac{\partial A(NL,NK)}{\partial K_x(L,M)} R(M) \\ &+ \sum_M \frac{\partial D(N,k)}{\partial A(NK,NL)} \frac{\partial A(NK,NL)}{\partial K_x(L,M)} R(M) \\ &+ \sum_M \frac{\partial D(N,k)}{\partial A(NK,NK)} \frac{\partial A(NK,NK)}{\partial K_x(L,M)} R(M) \end{aligned} \quad (\text{A-3})$$

- For (L,M) in the immediate vicinity of a Dirichlet boundary on the east, $K_x(L,M)$ appears only in $A(NK,NK)$, therefore, the right side of Equation A-2 for such $K_x(L,M)$ is

$$\text{Term I} = \sum_M \frac{\partial D(N,k)}{\partial A(NK,NK)} \frac{\partial A(NK,NK)}{\partial K_x(L,M)} R(M). \quad (\text{A-4})$$

For (L,M) representing location in the immediate vicinity of a Dirichlet boundary on the west

$$\text{Term I} = \sum_M \frac{\partial D(N,k)}{\partial A(NL,NL)} \frac{\partial A(NL,NL)}{\partial K_x(L,M)} R(M) \quad (\text{A-5})$$

In case the boundaries are of the Neumann type, $K_x(L,M)$ does not appear in any of the elements of [A] and

$$\text{Term I} = 0. \quad (\text{A-6})$$

The elements of matrix [A] are described in Equations 7 to 11. From these, it is apparent that for off-diagonal elements $A(NL,NK) = A(NK,NL)$

$$\frac{\partial A(NL,NK)}{\partial K_x(L,M)} = -r_w \frac{y(M+1/2) - y(M-1/2)}{x(L) - x(L-1)} = -ADIFX(L,M) \quad (\text{A-7})$$

For the diagonal element, on the other hand,

$$\frac{\partial A(NL,NL)}{\partial K_x(L,M)} = + ADIFX(L,M) \quad (\text{A-8})$$

Using Equations 24, A-7, and A-8, Equations A-4 to A-6 can be simplified to; respectively,

$$\text{Term I} = [H(NK) - H(NL)] \cdot [D(N,NL) - D(N,NK)] \cdot ADIFX(L,M) \quad (\text{A-9})$$

$$\text{Term I} = -D(N,NK) \cdot H(NK) \cdot ADIFX(L,M) \quad (\text{A-10})$$

$$\text{Term I} = -D(N,NL) \cdot H(NL) \cdot ADIFX(L,M). \quad (\text{A-11})$$

In Equations A-9 to A-11, H is obtained by multiplying matrix [D] with vector {R⁰}, where {R⁰} is formed by using expected values of the parameters.

Term II in Equations A-1 is

$$\text{Term II} = \sum_M D(N,k) \frac{\partial R(M)}{\partial K_x(L,M)} \quad (\text{A-12})$$

Again, we note the following characteristics of the discretized equations of PORSTAT.

- For (L,M) not in the immediate vicinity of the boundaries, $K_x(L,M)$ does not appear in any $R(M)$. Therefore, for such (L,M)

$$\text{Term II} = 0. \quad (\text{A-13})$$

- For (L,M) in the immediate vicinity of the boundaries, the way $K_x(L,M)$ appear in $R(M)$ depends on the kind of boundary condition.

For Dirichlet boundaries on the east, $K_x(L,M)$ appear in $R(NK)$ and for Dirichlet boundaries on the west in $R(NL)$ only and for these cases Term II can be found to be, respectively,

$$\text{Term II} = D(N,NK) \cdot \text{ADIFX}(L,M) \cdot \text{WBC}(M) \quad (\text{A-14})$$

$$\text{Term II} = D(N,NL) \cdot \text{ADIFX}(L,M) \cdot \text{EBC}(M) \quad (\text{A-15})$$

The expected boundary values on the west and east boundaries are WBC and EBC, respectively.

For the Neumann boundaries, the boundary hydraulic conductivities $K_x(L,M)$ do not appear in any $R(M)$, therefore,

$$\text{Term II} = 0. \quad (\text{A-16})$$

In summary, the following equations for computing $\partial h(I,J)/\partial K_x(L,M)$ are obtained:

- For $K_x(L,M)$ representing hydraulic conductivities at locations that are not in the immediate vicinity of any of the boundaries,

$$\frac{\partial h(N)}{\partial K_x(L,M)} = [H(NK) - H(NL)] \cdot [D(N,NL) - D(N,NK)] \cdot ADIFX(L,M). \quad (A-17)$$

- For $K_x(L,M)$ representing hydraulic conductivities at locations that are in the immediate vicinity of the boundary on the west,

$$\frac{\partial h(N)}{\partial K_x(L,M)} = [WBC(M) - H(NK)] \cdot D(N,NK) \cdot ADIFX(L,M) \quad (A-18)$$

for Dirichlet boundaries, and

$$\frac{\partial h(N)}{\partial K_x(L,M)} = 0 \quad (A-19)$$

for Neumann boundaries.

- For $K_x(L,M)$ representing hydraulic conductivities at locations that are in the immediate vicinity of the east boundary,

$$\frac{\partial h(N)}{\partial K_x(L,M)} = [EBC(M) - H(NL)] \cdot D(N,NL) \cdot ADIFX(L,M) \quad (A-20)$$

for Dirichlet boundaries, and

$$\frac{\partial h(N)}{\partial K_x(L,M)} = 0 \quad (A-21)$$

for Neumann boundaries.

A.3 SENSITIVITY COEFFICIENTS WITH RESPECT TO K_y

The derivation of equations for $\partial h(I,J)/\partial K_y(L,M)$ is similar to the ones for $\partial h(I,J)/\partial K_x(L,M)$ given above. Using new definitions of NL and NK and of ADIFY as given below,

$$NL = (L-2) \times IMAX1 + M-2 \quad (A-22)$$

$$NK = (L-2) \times IMAX1 + M-1 \quad (A-23)$$

$$ADIFY = [x(I+1/2)-x(I-1/2)]/[y(J)-y(J-1)] \quad (A-24)$$

the following equations for $\partial h(I,J)/\partial K_y(L,M)$ are obtained.

- For (L,M) not immediately adjacent to the boundaries,

$$\frac{\partial h(N)}{\partial K_y(L,M)} = [H(NK) - H(NL)] \cdot [D(N,NL) - D(N,NK)] \cdot ADIFY(L,M) \quad (A-25)$$

- For (L,M) in the immediate vicinity of the south boundary,

$$\frac{\partial h(N)}{\partial K_y(L,M)} = [SBC(L) - H(NK)] \cdot D(N,NK) \cdot ADIFY(L,M) \quad (A-26)$$

for Dirichlet boundaries, and

$$\frac{\partial h(N)}{\partial K_y(L,M)} = 0 \quad (A-27)$$

for Neumann-type boundaries.

- For (L,M) in the immediate vicinity of the north boundary,

$$\frac{\partial h(N)}{\partial K_y(L,M)} = [NBC(L) - H(NL)] \cdot D(N,NL) \cdot ADIFY(L,M) \quad (A-28)$$

for Dirichlet boundaries, and

$$\frac{\partial h(N)}{\partial R_y(L,M)} = 0 \quad (A-29)$$

for Neumann boundaries.

SBC and NBC in Equations A-28 and A-29 are the expected values of the Dirichlet conditions on the south and north boundaries, respectively.

A.4 SENSITIVITY COEFFICIENTS WITH RESPECT TO SPECIFIC STORAGE

An examination of the discretized equations of PORSTAT would reveal that the specific storage $S_s(L,M)$ occurs only in the element $A(NK,NK)$ and the right-hand vector element $R(NK)$, where $NK = (L-2) \times NOJ + M-1$.

Therefore, following the development in Section A.1

$$\frac{\partial h(N)}{\partial S_s(L,M)} = \frac{D(N,NK)}{\Delta t} [h^0(NK) - h(NK)] \quad (A-30)$$

where

Δt = the time step

h^0 = the value of the hydraulic head at the previous time step.

When a numerical procedure is followed, in which the steady state is obtained in a single step, $\Delta t \rightarrow \infty$, and $\partial h(N)/\partial S_s(L,M)$ is zero.

A.5. SENSITIVITY COEFFICIENTS WITH RESPECT TO BOUNDARY VALUES

In PORSTAT, boundary conditions are included in an implicit manner; i.e., the known boundary conditions are substituted in the discretized equations and transferred to the right-hand side (see Sec. 3.3.3). Thus, the boundary conditions appear only in the right-hand vector $\{R\}$, so that,

$$\frac{\partial h(N)}{\partial WBC(K)} = \sum_M D(N,M) \frac{\partial R(M)}{\partial WBC(K)} \quad (A-31)$$

If WBC(K) is of Dirichlet type, then

$$\frac{\partial h(N)}{\partial WBC(K)} = D(N, NK) \cdot K_x(2, K) \cdot ADIFX(2, K) \quad (A-32)$$

where

$$NK = K-1.$$

If WBC(K) is of Neumann type, then

$$\frac{\partial h(N)}{\partial WBC(K)} = [y(K+1/2) - y(K-1/2)] \quad (A-33)$$

The equations for first-order derivatives with respect to the other boundary conditions are very similar and are not written here.

A.6 SENSITIVITY COEFFICIENTS WITH RESPECT TO INITIAL CONDITIONS

In this discussion, by initial condition is meant the hydraulic head at the beginning of the new time step and is represented by HOLD (K,M). This variable, like the boundary conditions, appears only in the right-hand vector so that

$$\frac{\partial h(N)}{\partial HOLD(L, M)} = \sum_M D(N, M) \frac{\partial R(M)}{\partial HOLD(K, M)} \quad (A-34)$$

$$= D(N, NK) \cdot S(L, M) / \Delta t \quad (A-35)$$

where

$$NK = (L-2) \times NOJ + M-1$$

Δt = the time step.

APPENDIX B

EQUATIONS FOR SECOND-ORDER DERIVATIVES

B.1 INTRODUCTION

Second-order derivatives of the hydraulic head with respect to the uncertain parameters are required for the computation of the expected value of the hydraulic head. The equations for these derivatives are obtained by further differentiating the equations of sensitivity coefficients obtained in Appendix A. It should be noted that since {h} depends linearly on the initial and boundary conditions, therefore, the second-order derivatives of {h} with respect to these variables are zero. There are three second-order derivatives with respect to the hydraulic conductivity: with respect to K_x , with respect to K_y , and the mixed partial. There is one second-order derivative with respect to specific storage. Equations for these four second derivatives are summarized below.

B.2 SECOND-ORDER DERIVATIVES WITH RESPECT TO HYDRAULIC CONDUCTIVITY

The second-order derivative with respect to K_x can be written as

$$\frac{\partial^2 h(N)}{\partial K_x(L',M') \partial K_x(L,M)} = \frac{\partial}{\partial K_x(L',M')} \left[\sum_M \frac{\partial D(N,M)}{\partial K_x(L,M)} R(M) + \sum_M D(N,M) \frac{\partial R(M)}{\partial K_x(L,M)} \right] \quad (B-1)$$

The quantity within the braces on the right-hand side of Equation B-1 is the first-order derivative, which was evaluated in Appendix A. It was noted there that this quantity depends on whether the location (L,M) represented a boundary or not. In the same manner, the final equations for the second-order derivatives shall also depend on location. To simplify Equation B-1, define

$$NL = (L-2) \times NOJ + M-1 \quad (B-2)$$

$$NM = (L-3) \times NOJ + M-1 \quad (B-3)$$

$$NL' = (L'-2) \times NOJ + M'-1 \quad (B-4)$$

$$NM' = (L'-3) \times NOJ + M'-1 \quad (B-5)$$

For (L', M') not on the boundary, the variable $K_x(L', M')$ occurs in four elements of $[A]$. These are $A(NL', NM')$, $A(NL', NL')$, $A(NM', NL')$, and $A(NM', NM')$. For such K_x , Equation B-1 reduces to

$$\begin{aligned} \frac{\partial^2 h(N)}{\partial K_x(L', M') \partial K_x(L, M)} = & \{ [D(NM', NM) - D(NM', NL) + D(NL', NL) \\ & - D(NL', NM)] \cdot [H(NM) - H(NL)] \cdot [D(N, NM') - D(N, NL')] \\ & + [D(NM', NM) - D(NM', NL) + D(NL', NL) \\ & - D(NL', NM)] \cdot [H(NM') - H(NL')] \cdot [D(N, NM) \\ & - D(N, NL)] \} \cdot \{ ADIFX(L, M) ADIFX(L', M') \}. \end{aligned} \quad (B-6)$$

The formulas for other locations are as follows.

For both (L, M) and (L', M') representing locations near the west boundary, the equation is

$$\begin{aligned} \frac{\partial^2 h(N)}{\partial K_x(L', M') \partial K_x(L, M)} = & \{ D(NL', NL) \cdot [H(NL) D(N, NL')] \\ & + H(NL') D(N, NL) - D(N, NL') WBC(M) \\ & - D(N, NL) WBC(M') \} \cdot \{ ADIFX(L, M) ADIFX(L', M') \}. \end{aligned} \quad (B-7)$$

For (L, M) representing a location near the west boundary and (L', M') representing a location near the east boundary, the equation is

$$\begin{aligned} \frac{\partial^2 h(N)}{\partial K_x(L', M') \partial K_x(L, M)} = & \{ D(NM', NL) \cdot [H(NL) D(N, NM')] \\ & + H(NM') D(N, NL) - D(N, NM') WBC(M) \\ & - D(N, NL) WBC(M') \} \cdot \{ ADIFX(L, M) ADIFX(L', M') \}. \end{aligned} \quad (B-8)$$

For both (L,M) and (L',M') representing locations near the east boundary, the equation becomes

$$\begin{aligned} \frac{\partial^2 h(N)}{\partial K_x(L',M') \partial K_x(L,M)} &= \{D(NM',NM) \cdot [H(NM)D(N,NM')] \\ &+ H(NM')D(N,NM) - D(N,NM')EBC(M) \\ &- D(N,NL)EBC(M')]\} \cdot \{ADIFX(L,M)ADIFX(L',M')\}. \quad (B-9) \end{aligned}$$

For (L,M) representing locations near the east boundary and (L',M') representing one near the west boundary, the equation is

$$\begin{aligned} \frac{\partial^2 h(N)}{\partial K_x(L',M') \partial K_x(L,M)} &= \{D(NL',NM) \cdot [H(NM)D(N,NL)] \\ &+ H(NL')D(N,NM) - D(N,NL')EBC(M) \\ &- D(N,NM)EBC(M')]\} \cdot \{ADIFX(L,M)ADIFX(L',M')\}. \quad (B-10) \end{aligned}$$

For (L,M) representing locations near the east boundary and (L',M') representing locations away from both the east and west boundaries, the equation becomes

$$\begin{aligned} \frac{\partial^2 h(N)}{\partial K_x(L',M') \partial K_x(L,M)} &= \{[D(NM',NM) - D(NL',NM)] \cdot H(NM) \cdot [D(N,NM) \\ &- D(N,NL')] + D(N,NM) \cdot [H(NM') - H(NL')] \\ &+ EBC(M) \cdot [D(N,NM')] \\ &- D(N,NL')]\} \cdot \{ADIFX(L,M)ADIFX(L',M')\}. \quad (B-11) \end{aligned}$$

For (L,M) representing locations near the west boundary and (L',M') representing location which are not in the immediate vicinity of either east or west boundary, the equation takes the form

$$\begin{aligned} \frac{\partial^2 h(N)}{\partial k_x(L',M') \partial k_x(L,M)} = & \{ [D(NM',NL) - D(NL',NL)] \cdot H(NL) \cdot [D(N,NM') \\ & - D(N,NL')] + D(N,NL) \cdot [H(NM') - H(NL')] \\ & + WBC(M) \cdot [D(N,NL) \\ & - D(N,NM')] \} \cdot \{ ADIFX(L,M) ADIFX(L',M') \}. \quad (B-12) \end{aligned}$$

For (L',M') representing locations near the west boundary and (L,M) representing locations not in the immediate vicinity of either the east and west boundary, the equation becomes

$$\begin{aligned} \frac{\partial^2 h(N)}{\partial k_x(L',M') \partial k_x(L,M)} = & \{ [D(NL',NM) - D(NL',NL)] \cdot H(NL') \cdot [D(N,NM) \\ & - D(N,NL)] + D(N,NL') \cdot [H(NM) - H(NL)] \\ & + WBC(M') \cdot [D(N,NL) \\ & - D(N,NM)] \} \cdot \{ ADIFX(L,M) ADIFX(L',M') \}. \quad (B-13) \end{aligned}$$

Finally, for (L',M') representing locations near the east boundary and (L,M) representing any location, which is neither in the immediate vicinity of the east or the west boundary, the equation is

$$\begin{aligned} \frac{\partial^2 h(N)}{\partial k_x(L',M') \partial k_x(L,M)} = & \{ [D(NM',NM) - D(NM',NL)] \cdot H(NM') \cdot [D(N,NM) \\ & - D(N,NL)] + D(N,NM') \cdot [H(NM) - H(NL)] \\ & + EBC(M') \cdot [D(N,NL) \\ & - D(N,NM)] \} \cdot \{ ADIFX(L,M) ADIFX(L',M') \}. \quad (B-14) \end{aligned}$$

Equations B-6 to B-14 can also be applied to finding the second-order derivative with respect to K_y , as well as to the mixed partial derivative, provided that the NL, NM, NL', and NM' are appropriately defined and the appropriate boundary conditions (i.e., SBC and NBC) are considered.

B.2 SECOND-ORDER DERIVATIVE WITH RESPECT TO SPECIFIC STORAGE

The equation for the second-order derivative with respect to specific storage is obtained by differentiating Equation A-30 once again with respect to S_s . The equation so obtained is

$$\frac{\partial^2 h(N)}{\partial S_s(L, M) \partial S_s(L', M')} = D(NL', NL) \{ D(N, NL') H(NL) + D(N, NL) H(NL') \} \Delta t^2 \quad (B-15)$$

where

$$NL = (L-2) \times NOJ + M-1 \quad (B-16)$$

$$NL' = (L'-2) \times NOJ + M'-1. \quad (B-17)$$

It should again be noted that in case a steady-state problem is to be solved in a single step, this second derivative with respect to specific storage would be zero.

APPENDIX C

EQUATIONS FOR COVARIANCE OF DARCIAN VELOCITIES

C.1 COVARIANCE OF U AND V

It was suggested in Section 3.6 that the Darcian velocities are functions of all of the uncertain variables. In view of this, we can expand the U and V functions of Equations 26 and 27 in a Taylor series and obtain an equation analogous to 19. In the following, only the equation for U is discussed. The equation of V is similar.

$$\begin{aligned}
 U(K,J) &= \tilde{U}(K,J) + [K_x(K,J) - \bar{K}_x(K,J)] \frac{\partial U(K,J)}{\partial K_x(K,J)} \\
 &+ [h(I-1,J) - \bar{h}(I-1,J)] \frac{\partial U(K,J)}{\partial h(I-1,J)} \\
 &+ [h(I,J) - \bar{h}(I,J)] \frac{\partial U(K,J)}{\partial h(I,J)} \tag{C-1}
 \end{aligned}$$

where

\tilde{U} = the value of U obtained by substituting the expected values of K_x and h in Equation 26.

A bar over a variable in Equation C-1 denotes its expected value. Taking expected value of both sides of Equation C-1, we get

$$U(K,J) = \tilde{U}(K,J). \tag{C-2}$$

To obtain covariance, we write an expression for $\{U(K,J)U(K',J')\}$, take its expected value and subtract $\{\bar{U}(K,J)\bar{U}(K',J')\}$. Thus,

$$\begin{aligned}
 \text{Cov}[U(K,J), U(K',J')] &= \text{Cov}[K_x(K,J), K_x(K',J')] \frac{\partial U(K,J)}{\partial K_x(K,J)} \frac{\partial U(K',J')}{\partial K_x(K',J')} \\
 &+ \text{Cov}[K_x(K,J), h(I'-1,J')] \frac{\partial U(K,J)}{\partial K_x(K,J)} \frac{\partial U(K',J')}{\partial h(I'-1,J')} \\
 &+ \text{Cov}[K_x(K,J), h(I',J')] \frac{\partial U(K,J)}{\partial K_x(K,J)} \frac{\partial U(K',J')}{\partial h(I',J')}
 \end{aligned}$$

$$\begin{aligned}
& + \text{Cov}[h(I-1, J), K_x(K', J')] \frac{\partial U(K, J)}{\partial h(I-1, J)} \frac{\partial U(K', J')}{\partial K_x(K', J')} \\
& + \text{Cov}[h(I-1, J), h(I'-1, J')] \frac{\partial U(K, J)}{\partial h(I-1, J)} \frac{\partial U(K', J')}{\partial h(I'-1, J')} \\
& + \text{Cov}[h(I-1, J), h(I', J')] \frac{\partial U(K, J)}{\partial h(I-1, J)} \frac{\partial U(K', J')}{\partial h(I', J')} \\
& + \text{Cov}[h(I, J), K_x(K', J')] \frac{\partial U(K, J)}{\partial h(I, J)} \frac{\partial U(K', J')}{\partial K_x(K', J')} \\
& + \text{Cov}[h(I, J), h(K'-1, J')] \frac{\partial U(K, J)}{\partial h(I, J)} \frac{\partial U(K', J')}{\partial h(K'-1, J')} \\
& + \text{Cov}[h(I, J), h(I', J')] \frac{\partial U(K, J)}{\partial h(I, J)} \frac{\partial U(K', J')}{\partial h(I', J')} \tag{C-3}
\end{aligned}$$

where, all the derivatives are evaluated at the expected values of the parameters involved. That is,

$$\frac{\partial U(K, J)}{\partial K_x(K, J)} = [h(I-1, J) - h(I, J)] / \text{DXM}(I) = \text{DK1} \tag{C-4}$$

$$\frac{\partial U(K, J)}{\partial h(I-1, J)} = K_x(K, J) / \text{DXM}(I) = \text{DP1} \tag{C-5}$$

$$\frac{\partial U(K, J)}{\partial h(I, J)} = -K_x(K, J) / \text{DXM}(I) = -\text{DP1} \tag{C-6}$$

where

$$\text{DXM}(I) = x(I+1/2) - x(I-1/2).$$

DK2 and DP2, the derivatives of $U(K', J')$, can similarly be defined.

To evaluate Equation C-3, we need an equation for $\text{Cov}[K_x(M, N), h(I, J)]$ that can again be obtained up to second-order as follows.

The product $[K_x(M,N) h(I,J)]$ may be written as

$$\begin{aligned}
 K_x(M,N) h(I,J) &= K_x(M,N) h(I,J) \\
 &+ \sum_M \sum_N 0.5[K_x(M,N) - \bar{K}_x(M,N)] \cdot K_x(M,N) \frac{\partial^2 h(I,J)}{\partial K_x^2(M,N)} \\
 &+ 2 \frac{\partial h(I,J)}{\partial K_x(M,N)} + \sum_M \sum_N 0.5[S_s(M,N) \\
 &- S_s(M,N)] \cdot K_x(M,N) \frac{\partial^2 h(I,J)}{\partial S_s^2(M,N)} + \frac{\partial h(I,J)}{\partial S_s(M,N)} + \dots \quad (C-7)
 \end{aligned}$$

Note that the second-order derivatives $\{h\}$ with respect to boundary conditions and initial condition are zero and these terms, therefore, are not shown in Equation C-7. Similarly, all the first-order terms are omitted since these become zero on taking their expectation. Taking the expected value of both sides of Equation C-7, the covariance of $[K_x(M,N), h(I,J)]$ can be obtained as

$$\begin{aligned}
 \text{Cov}[K_x(M,N), h(I,J)] &= 1/2 \text{Var}[K_x(M,N)] \cdot [\bar{K}_x(M,N) \frac{\partial^2 h(I,J)}{\partial K_x^2(M,N)} \\
 &+ 2 \frac{\partial h(I,J)}{\partial K_x(M,N)}] + 1/2 \text{Var}[S_s(M,N)] \cdot [\bar{K}_x(M,N) \frac{\partial^2 h(I,J)}{\partial S_s^2(M,N)} \\
 &+ \frac{\partial h(I,J)}{\partial S_s(M,N)}] \quad (C-8)
 \end{aligned}$$

Equations for the first- and second-order derivatives of $\{h\}$ with respect to K_x and S have already been developed in Appendices A and B. Using Equation C-8, the covariance function of U can be evaluated from Equation C-3.

APPENDIX D

MONTE CARLO TECHNIQUE FOR ANALYZING UNCERTAINTIES IN HYDRAULIC HEADS

The Monte Carlo method used by MAGNUM-MC to analyze uncertainties in hydraulic head predictions is the same method described by Clifton and Neuman (1982). With this method, the hydraulic conductivity field within the modeled domain is assumed to be governed by a log-normal probability distribution. Following discretization of the conductivity field, which is required by the finite-element numerical scheme used by MAGNUM-MC, a mean vector and covariance matrix must be determined for the field. A multivariate normal random number generator is then used to generate a large number of random conductivity fields having the same covariance structure. The number of random fields needed to assure convergence of the statistics of the ensemble is determined by the two norms defined in Equations 58 and 59 of Clifton and Neuman (1982). In Test Cases 1 and 2 of this study, 400 simulations were determined to be sufficient to obtain reliable statistics of the ensemble of random hydraulic conductivity fields. The ensemble of conductivity fields is then input to MAGNUM-MC to generate the corresponding ensemble of random hydraulic head fields. Statistics of these head fields at each node of the finite-element mesh can readily be determined.

REFERENCE

- Clifton, P. M. and Neuman, S. P., 1982, "Effects of Kriging and Inverse Modeling on Conditional Simulation of the Avra Valley Aquifer in Southern Arizona," Water Resources Research, Vol. 18, No. 4, pp. 1215-1234.

APPENDIX E

HYDRAULIC CONDUCTIVITY FIELD MEAN VECTOR AND COVARIANCE
MATRIX GENERATION, TEST CASE 1

The hydraulic conductivity (K) fields input to PORSTAT and MAGNUM-MC in Test Case 1 were isotropic and homogeneous, and were assumed to be governed by a log-normal probability distribution. The geometric mean of K and the variance of log-hydraulic conductivity (log-K) were set at 1×10^{-6} m/sec (= 31.5 m/yr) and 0.1, respectively.

The complement of the spherical semivariogram model (Journel and Huijbregts, 1978) was used to describe the covariance structure of log-K in the model domains used by PORSTAT and MAGNUM-MC. Relevant parameters of this model were: sill 0.1, and x-direction range 3,500 m. In addition, the covariance structure was assumed to be anisotropic, with the ratio of the ranges in the x- and y-directions being 2.

The grid used to define the log-K covariance matrix for PORSTAT was a modified version of the grid in Figure 4. Modification of this grid was required because of the way K's are input to PORSTAT. As explained in Section 3.0 (Eq. 7 to 11) PORSTAT requires the K's to be defined between adjacent nodes of the mesh rather than at the nodes. The result is two separate meshes for the x- and y-direction K's. These meshes, together with the internal grid nodes, are shown in Figure E-1. Each cell of the meshes is a finite subregion where K is defined. The x- and y-direction log-K covariance matrices were obtained by integrating the log-K covariance function around each mesh. In addition, the x- and y-direction log-K's were assumed to be uncorrelated.

PORSTAT requires the expected value and covariance matrix of K rather than log-K. The transformation described in Appendix G was used to derive the expected value vector and covariance matrix of K.

In order to use the multivariate normal random number generator (Appendix D) to develop the suite of random K fields for MAGNUM-MC, a mean vector and covariance matrix of log-K are required. The mean vector used in this test case had every element equal to the logarithm of the geometric mean of K (i.e., $\log_{10}(31.5)$). The log-K covariance matrix was developed by integrating the log-K covariance function around the mesh in Figure 4. As explained in the test, this mesh has the same geometry as the mesh used by MAGNUM-MC.

REFERENCE

Journel, A. G. and Huijbregts, Ch. J., 1978, Mining Geostatistics, Academic Press, New York, New York.

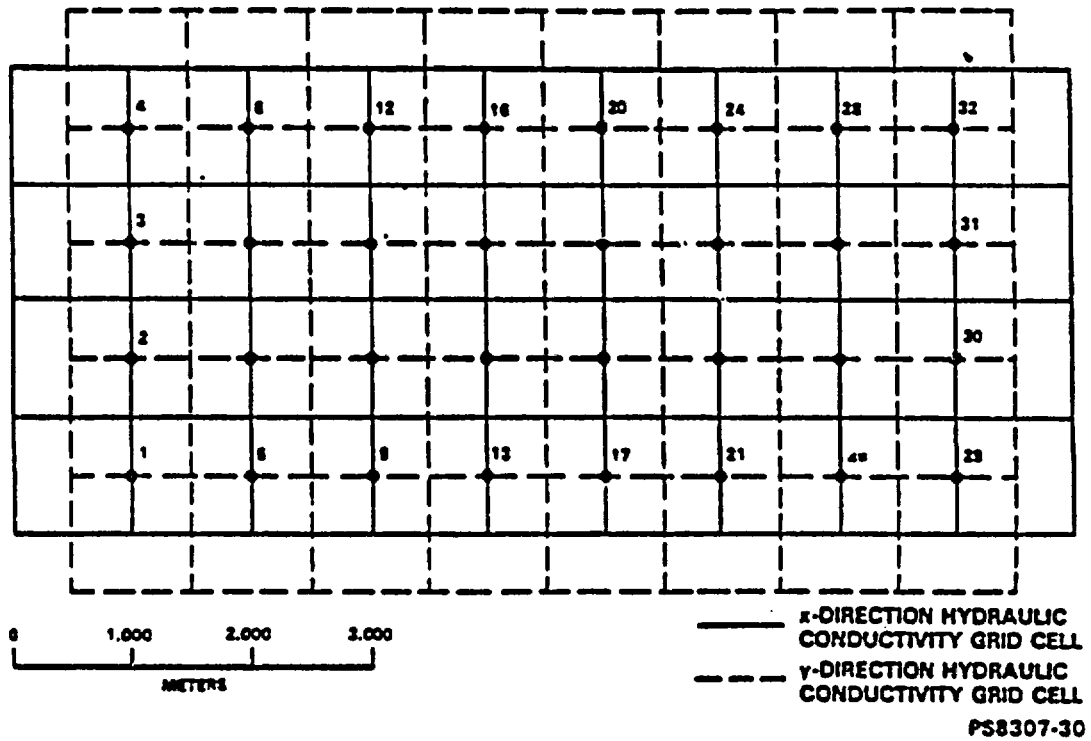


FIGURE E-1. Grid System Used by PORSTAT to Define x- and y-direction Hydraulic Conductivities. Grid nodes correspond with nodes in Figure 4.

APPENDIX F

HYDRAULIC CONDUCTIVITY FIELD MEAN VECTOR AND COVARIANCE
MATRIX GENERATION, TEST CASE 2

The hydraulic conductivity (K) fields input to PORSTAT and MAGNUM-MC in Test Case 2 were isotropic, heterogeneous, and had a nonuniform covariance structure. These fields were assumed to be governed by a log-normal probability distribution. The same mesh geometries that were used in Test Case 1 were also used in Test Case 2. In order to generate the desired K fields, 60 synthetic, randomly-distributed log-hydraulic conductivity (log-K) data with a specified covariance structure were first generated in the 5,000-m by 9,000-m domain containing the PORSTAT and MAGNUM-MC meshes. These data were generated by means of the multivariate normal random number generator described by Clifton and Neuman (1982). The covariance structure of the synthetic log-K data was defined by the spherical semivariogram model (Journel and Huijbregts, 1978) with parameters: sill 0.65, and x-direction range 3,500 m. In addition, the covariance structure was assumed to be anisotropic, with the ratio of the ranges in the x- and y-directions being 2. The geostatistical interpolation technique of kriging was then used to make estimates of log-K in each of the cells of the meshes, and also to determine the log-K covariance matrix for each mesh (Clifton and Neuman, 1982). By using kriging to condition the estimates of log-K in each cell, a heterogeneous log-K field with a nonuniform covariance structure as generated. The transformation described in Appendix G was used to obtain the expected value vector and covariance matrix for K required by PORSTAT.

REFERENCES

- Clifton, P. M. and Neuman, S. P., 1982, "Effects of Kriging and Inverse Modeling on Conditional Simulation of the Avra Valley Aquifer in Southern Arizona," Water Resources Research, Vol. 18, No. 4, pp. 1215-1234.
- Journel, A. G. and Huijbregts, Ch. J., 1978, Mining Geostatistics, Academic Press, New York, New York.

APPENDIX G

DERIVATION OF THE MEAN VECTOR AND COVARIANCE MATRIX OF A LOG-NORMALLY DISTRIBUTED RANDOM VARIABLE GIVEN THE MEAN VECTOR AND COVARIANCE MATRIX OF THE CORRESPONDING NORMALLY DISTRIBUTED RANDOM VARIABLE

Let \underline{Y} be a vector of normally distributed random variables with mean $E[\underline{Y}]$ and covariance matrix \underline{V}_Y ; i.e., \underline{Y} is $N(E[\underline{Y}], \underline{V}_Y)$.

Let

$$\underline{Y} = \log_a(\underline{K})$$

then \underline{K} is a vector of log-normally distributed random variables, and

$$\underline{K} = \exp(c\underline{Y})$$

where

$$c = \ln(a).$$

The mean and variance of \underline{K} are given by, respectively (Benjamin and Cornell, 1970),

$$E[K_i] = \exp(cE[Y_i] + 0.5c^2V_{Y_{ii}})$$

$$V_{K_{ii}} = (E[K_i])^2[\exp(c^2V_{Y_{ii}}) - 1].$$

The covariance matrix of \underline{K} is given by (Benjamin and Cornell, 1970)

$$\text{Cov}[K_i, K_j] = E[K_i K_j] - E[K_i]E[K_j].$$

Expanding the first term on the right of the above equation yields:

$$\begin{aligned} E[K_i K_j] &= E[\exp(cY_i) \cdot \exp(cY_j)] \\ &= E[\exp(cY_i + cY_j)]. \end{aligned}$$

Since cY_1 and cY_2 are two normal random variables, their sum is also normal.
Thus

$$\begin{aligned} E[K_1 K_2] &= \exp\{c(E[Y_1] + E[Y_2]) + 0.5c^2 \text{Var}(Y_1 + Y_2)\} \\ &= \exp\{c(E[Y_1] + E[Y_2]) + c^2(0.5V_{Y11} + 0.5V_{Y22} \\ &\quad + \text{Cov}[Y_1, Y_2])\}. \end{aligned}$$

Hence the covariance matrix of \underline{K} is given by

$$\begin{aligned} \text{Cov}[K_1, K_2] &= \exp\{c(E[Y_1] + E[Y_2]) + c^2(0.5V_{Y11} + 0.5V_{Y22} \\ &\quad + \text{Cov}[Y_1, Y_2])\} - \exp(cE[Y_1] + 0.5c^2V_{Y11}) \cdot \exp(cE[Y_2] \\ &\quad + 0.5c^2V_{Y22}) \\ &= \exp\{c(E[Y_1] + E[Y_2]) + 0.5c(V_{Y11} \\ &\quad + V_{Y22})\} \cdot (\exp(c^2 \text{Cov}[Y_1, Y_2]) - 1) \\ &= E[K_1]E[K_2] \cdot (\exp(c^2 \text{Cov}[Y_1, Y_2]) - 1). \end{aligned}$$

REFERENCE

Benjamin, J. R. and Cornell, C. A., 1970, Probability, Statistics, and Decision for Civil Engineers, McGraw-Hill Book Company, New York, New York.

DISTRIBUTION

Number of copiesOFFSITE

6	<u>Analytical and Computational Research, Inc.</u> A. K. Runchal B. Sagar (5)
2	<u>Arizona State University</u> J. R. Holloway
1	<u>Arthur D. Little, Inc.</u> C. R. Hadlock
2	<u>Atomic Energy of Canada Research Company</u> E. L. J. Rosinger B. J. S. Wilkins
11	<u>Battelle-Office of Nuclear Waste Isolation</u> S. J. Basham S. C. Mathews A. Brandstetter W. E. Newcomb S. Gupta Library (5) P. L. Hofmann
1	<u>Boeing Commercial Airplane Co.</u> K. Ekblad
2	<u>Creek Geotechnical Engineering</u> B. Y. Kanehiro C. R. Wilson
1	<u>D'Appolonia Consulting Engineers, Inc.</u> J. B. Case
1	<u>GeoTran, Inc.</u> P. Hyakorn
1	<u>Holcomb Research Institute</u> N. Vesper

Number of copies

1	<u>Institute for Tieflagerung</u> E. Uerpmann
1	<u>ISMES</u> F. Gera
2	<u>Lawrence Berkeley Laboratory</u> T. N. Narasimhan Library
3	<u>Lawrence Livermore National Laboratory</u> D. Isherwood W. C. Patrick Library
2	<u>Los Alamos National Laboratory</u> B. Crowe Library
1	<u>Massachusetts Institute of Technology</u> L. W. Gelhar
1	<u>NAGRA - National Cooperative for the Storage of Radioactive Waste</u> C. McCombie
2	<u>National Radiological Protection Board</u> P. D. Grimwood M. D. Hill
1	<u>Nuclear Energy Agency</u> P. Johnston
2	<u>Princeton University</u> G. F. Pinder Library
1	<u>Resource Management Associates</u> I. P. King

Number of copies

1 Ontario Hydro
K. K. Tsui

8 Sandia National Laboratories
R. M. Cranwell M. Reade
R. W. Lynch A. E. Stephenson
J. W. Nunciato L. D. Tyler
R. E. Pepping Library

*5 Siting/Licensing Overview Committee
P. Domenico
F. Parker
H. Ross
J. Smith
D. Swanson

1 Science Applications, Inc.
L. Rickertsen

2 Stanford University
I. Remson
Library

*1 State of Texas Attorney General's Office
M. Plaster

1 The Analytical Sciences Corporation
J. W. Bartlett

1 U.S. Department of Energy-
Columbus Program Office
J. O. Neff

*3 U.S. Department of Energy-Headquarters
W. W. Ballard, Jr.
M. W. Frei
R. Stein

1 U.S. Department of Energy-
Nevada Operations Office
D. L. Vieth

Number of copies

1	<u>U.S. Department of Energy-Public Reading Room</u> Seattle, Washington
2	<u>U.S. Environmental Protection Agency</u> Headquarters Library Region X Library
2	<u>U.S. Geological Survey</u> D. B. Grove K. L. Kipp
10	<u>U.S. Nuclear Regulatory Commission</u> M. Gordon M. Knapp Branch Chief, High-Level Waste Technical Development Branch* Branch Chief, High-Level Waste Licensing Management Branch* Director, Division of Waste Management* Docket Control Center-Division of Waste Management (4)* Library*
2	<u>University of Arizona</u> S. P. Neuman Library
1	<u>University of Waterloo</u> E. O. Frind
3	<u>Washington State Department of Ecology</u> D. W. Moos (2)* Library
1	<u>Washington State Department of Natural Resources</u> Library
<u>ONSITE</u>	
1	<u>BCS Richland, Inc.</u> N. W. Kline

Number of copies

7

Pacific Northwest Laboratory

H. C. Burkholder R. W. Nelson
C. R. Cole A. E. Reisenauer
F. H. Dove Library
B. Kuhn

1

U.S. Department of Energy-
Richland Operations Office

O. L. Olson

29

Rockwell Hanford Operations

R. C. Arnett
R. G. Baca
P. M. Clifton (5)
R. A. Deju
R. T. Wilde
Basalt Waste Isolation Project Library (15)*
Document Control (2)*
Publications Services Department-Station 2 (2)*
Records Retention*